Journal of Computational Physics 330 (2017) 340–364

Contents lists available at ScienceDirect

Journal of Computational Physics

www.elsevier.com/locate/jcp

Discontinuous Galerkin methods for Hamiltonian ODEs and PDEs

Wensheng Tang [a], Yajuan Sun [b,c,*], Wenjun Cai [d]

[a] College of Mathematics and Statistics, Changsha University of Science and Technology, Changsha 410114, China
[b] LSEC, Academy of Mathematics and Systems Science, Chinese Academy of Sciences, Beijing 100190, China
[c] University of Chinese Academy of Sciences, Beijing 100049, China
[d] Laboratory of Computational Geodynamics, Chinese Academy of Sciences, Beijing 100049, China

ARTICLE INFO

Article history:
Received 24 November 2015
Received in revised form 4 October 2016
Accepted 16 November 2016
Available online 22 November 2016

Keywords:
Discontinuous Galerkin method
Hamiltonian systems
Continuous-stage PRK method
Symplectic PRK scheme
Multi-symplectic PRK scheme
Conservation laws

ABSTRACT

In this article, we present a unified framework of discontinuous Galerkin (DG) discretizations for Hamiltonian ODEs and PDEs. We show that with appropriate numerical fluxes the numerical algorithms deduced from DG discretizations can be combined with the symplectic methods in time to derive the multi-symplectic PRK schemes. The resulting numerical discretizations are applied to the linear and nonlinear Schrödinger equations. Some conservative properties of the numerical schemes are investigated and confirmed in the numerical experiments.

1. Introduction

Studying the geometric properties of dynamical systems and constructing the corresponding numerical algorithms based on these geometric properties have drawn much attention of mathematicians and scientists during these years. The numerical discretization which can inherit the geometric properties of the original systems is referred to as geometric numerical integration or structure-preserving algorithm in the literature [9,10]. The backward error analysis [10] states that the numerical discretization with conservative properties will generally help to produce the numerical solutions with improved qualitative behavior. This allows the numerical simulations to be more stable and accurate than those computed by traditional methods especially in the long-time integration. Due to the advantage, the structure-preserving algorithms have been developed rapidly in recent years. They include symplectic methods for Hamiltonian systems, symmetric methods for reversible systems, invariant-preserving methods for conservative systems with constants of motion, volume-preserving methods for source-free systems, numerical methods on manifolds etc. (see [9,10] and the references therein). Among them symplectic methods have been systematically investigated since 1980s for solving Hamiltonian ordinary differential equations (ODEs) [9,10]. By the method of line approach [20], symplectic methods can also be applied to Hamiltonian partial differential equations (PDEs). Differently from the infinite dimensional Hamiltonian system description, by introducing the bundle coordinates Marsden et al. [19] and Bridges & Reich [4] have independently proposed the concept of multi-symplectic geometry for reformulating Hamiltonian PDEs. In this framework, the system of Hamiltonian PDEs is defined on a finite di-

* Corresponding author at: LSEC, Academy of Mathematics and Systems Science, Chinese Academy of Sciences, Beijing 100190, China.
E-mail addresses: tangws@lsec.cc.ac.cn (W. Tang), sunyj@lsec.cc.ac.cn (Y. Sun), wenjuncai1@gmail.com (W. Cai).

http://dx.doi.org/10.1016/j.jcp.2016.11.023
0021-9991/

mensional bundle space, and its multi-symplectic structure can be viewed as a generalization of symplectic structure in time and space. A numerical method is called multi-symplectic if it can preserve the discrete multi-symplectic conservation law. For more details, please see [4,19,12,13,27,23,32] and the references therein.

There are various ways in order to construct the geometric numerical integration for Hamiltonian system, e.g. the variational method, the generating function approach, the Runge–Kutta method. All these methods are based on the Hamiltonian formulation of the system. It is noticed recently that a completely different approach has been developed based on the Galerkin variational formulation of the system. With the introduction of finite element methods [2,3,15], the resulting discretizations can be related to symplectic methods and energy-preserving methods [1,5,29,17].

In this paper, we mainly focus on employing the discontinuous Galerkin (DG) method (one kind of non-standard finite element methods (FEMs)) for solving Hamiltonian ODEs and PDEs. We firstly investigate the DG discretization for Hamiltonian ODEs, and show that the resulting algorithm can be related to high-order symplectic partitioned Runge–Kutta (PRK) scheme. Then, we consider the DG discretization for the conservative PDEs written in multi-symplectic formulation, and reveal its connection to multi-symplectic PRK scheme.

The outline of this paper is as follows. In the next section, we introduce the general framework of the DG approach and PRK discretization for the first order PDEs. In section 3, we consider the Hamiltonian system and apply the DG approach in order to design the symplectic methods. Section 4 is devoted to discretizing Hamiltonian PDEs in the DG framework, and connecting to the multi-symplectic methods. In section 5, we take the nonlinear Schrödinger equation as a model problem and investigate the geometric-structure preservation of the corresponding discretization. We present numerical experiments in section 6. At last, we conclude this paper with some remarks.

2. Discontinuous Galerkin approach and PRK discretization

In this section, we introduce the DG approach and PRK discretization for solving the first order PDEs, and establish the connection between DG and PRK discretizations.

2.1. Discontinuous Galerkin approach

The first DG method was proposed in 1973 by Reed and Hill [21] for solving the linear hyperbolic equations in neutron transport. Since the DG method uses the discontinuous piecewise polynomials as the basis functions, it is taken as a kind of non-standard finite element method (see [7,25] and the references therein for more details).

Let us start to introduce the DG method by considering the following one-dimensional first order equation in conservation law form [25]

$$u_t + f(u)_x = 0, \quad x \in \Omega = [\mathcal{L}, \mathcal{R}]. \tag{2.1}$$

Divide Ω as $\Omega = \bigcup_{j=0}^{N-1}[x_j, x_{j+1}]$ with $x_0 = \mathcal{L}$ and $x_N = \mathcal{R}$, and denote $\Omega_j = [x_j, x_{j+1}],\ j = 0, 1, \cdots, N-1$. We define the space of piecewise polynomial functions by

$$V_{\Delta x}^k(\Omega) = \{\chi :\ \chi|_{\Omega_j} \in \mathbb{P}^k(\Omega_j),\ 0 \le j \le N-1\},$$

where $\Delta x = \max_j\{\Delta x_j :\ \Delta x_j = x_{j+1} - x_j\}$, $\mathbb{P}^k$ denotes the set of polynomials of degree up to k. Note that the functions in $V_{\Delta x}^k(\Omega)$ are allowed to be discontinuous across the element interfaces. Then, the weak form for the DG method applied to system (2.1) is

$$\int_{\Omega_j} U_t \phi \mathrm{d}x - \int_{\Omega_j} f(U)\phi_x \mathrm{d}x + \widehat{f}_{j+1}\phi_{j+1}^- - \widehat{f}_j \phi_j^+ = 0,\ 0 \le j \le N-1, \tag{2.2}$$

where $U, \phi \in V_{\Delta x}^k(\Omega)$ [7]. In the above equality, ϕ is the test function with ϕ_j^+ and ϕ_j^- the right and left limit values of ϕ at x_j, respectively, and $\widehat{f}_j$ denotes the numerical flux (it is usually a single valued function) at element interfaces in order to ensure the consistency, continuity and monotonicity of the resulting discretizations [7].

The DG approach can also be able to be applied to discretize the PDEs with higher order derivatives by rewriting the PDEs into a first order system [34]. For example, by introducing an auxiliary variable v, the heat equation $u_t - u_{xx} = 0$ can be augmented as a first order system $u_t - v_x = 0,\ v - u_x = 0$. This, in turn, allows us to apply the DG approach and derive the following discretization for solving the heat equation

$$\int_{\Omega_j} (U_t\phi + V\phi_x)\,\mathrm{d}x - \widehat{V}_{j+1}\phi_{j+1}^- + \widehat{V}_j\phi_j^+ = 0, \int_{\Omega_j} (V\psi + U\psi_x)\,\mathrm{d}x - \widehat{U}_{j+1}\psi_{j+1}^- + \widehat{U}_j\psi_j^+ = 0,$$

where $U, V, \phi, \psi \in V_{\Delta x}^k(\Omega)$ and ϕ, ψ are the test functions.

2.2. Partitioned Runge–Kutta discretization

In this subsection, we review the Partitioned Runge–Kutta (PRK) discretization by starting with the d-dimensional system of ODEs

$$\boldsymbol{z}_t = \boldsymbol{f}(t, \boldsymbol{z}), \qquad \boldsymbol{z}(t_0) = \boldsymbol{z}_0.$$

In order to introduce the PRK method, we partition the above system into several parts

$$\boldsymbol{z}_t^{(\gamma)} = \boldsymbol{f}^{(\gamma)}(t, \boldsymbol{z}) \in \mathbb{R}^{d_\gamma}$$

with $\sum_{\gamma=1}^{\alpha} d_\gamma = d$. We apply an s-stage RK discretization denoted by $(a_{ij}^{(\gamma)}, b_i^{(\gamma)}, c_i^{(\gamma)}, 1 \le i, j \le s)$ to each $\boldsymbol{z}^{(\gamma)}$ $(1 \le \gamma \le \alpha)$, it provides the following s-stage PRK scheme [23]

$$\begin{aligned} \boldsymbol{Z}_i^{(\gamma)} &= \boldsymbol{z}_0^{(\gamma)} + \Delta t \sum_{j=1}^{s} a_{ij}^{(\gamma)} \partial_t \boldsymbol{Z}_j^{(\gamma)}, \\ \boldsymbol{z}_1^{(\gamma)} &= \boldsymbol{z}_0^{(\gamma)} + \Delta t \sum_{i=1}^{s} b_i^{(\gamma)} \partial_t \boldsymbol{Z}_i^{(\gamma)}, \end{aligned} \tag{2.3}$$

where the new variables $\partial_t \boldsymbol{Z}_j^{(\gamma)}$ and the stage values $\boldsymbol{Z}_j = (\boldsymbol{Z}_j^{(1)}, \cdots, \boldsymbol{Z}_j^{(\alpha)})$ satisfy

$$\partial_t \boldsymbol{Z}_j^{(\gamma)} = \boldsymbol{f}^{(\gamma)}(t_0 + c_j^{(\gamma)} \Delta t, \boldsymbol{Z}_j), \ \ 1 \le j \le s, \ 1 \le \gamma \le \alpha \tag{2.4}$$

with $\boldsymbol{Z}_j^{(\gamma)} \approx \boldsymbol{z}(t_0 + c_j^{(\gamma)} \Delta t)$, $\boldsymbol{z}_1^{(\gamma)} \approx \boldsymbol{z}^{(\gamma)}(t_0 + \Delta t)$ and $\boldsymbol{z}_0^{(\gamma)}$ the initial value.

Moreover, we consider the multi-symplectic Hamiltonian system

$$M \boldsymbol{z}_t + K \boldsymbol{z}_x = \nabla_{\boldsymbol{z}} S(\boldsymbol{z})$$

(see also (4.1)). When apply an r-stage PRK method and an s-stage PRK method to discretize the time and space variables, respectively, we get the time-space PRK discretization [12,23,27]

$$\begin{aligned} &\boldsymbol{Z}_{ij}^{(\gamma)} = \boldsymbol{z}_j^{(\gamma)0} + \Delta t \sum_{\iota=1}^{r} a_{i\iota}^{(\gamma)} \partial_t \boldsymbol{Z}_{\iota j}^{(\gamma)}, \ \ \boldsymbol{z}_j^{(\gamma)1} = \boldsymbol{z}_j^{(\gamma)0} + \Delta t \sum_{\iota=1}^{r} b_\iota^{(\gamma)} \partial_t \boldsymbol{Z}_{\iota j}^{(\gamma)}, \\ &\boldsymbol{Z}_{ij}^{(\gamma)} = \boldsymbol{z}_0^{(\gamma)i} + \Delta x \sum_{\iota=1}^{s} \widetilde{a}_{j\iota}^{(\gamma)} \partial_x \boldsymbol{Z}_{i\iota}^{(\gamma)}, \ \ \boldsymbol{z}_1^{(\gamma)i} = \boldsymbol{z}_0^{(\gamma)i} + \Delta x \sum_{\iota=1}^{s} \widetilde{b}_\iota^{(\gamma)} \partial_x \boldsymbol{Z}_{i\iota}^{(\gamma)}, \\ &M \partial_t \boldsymbol{Z}_{ij} + K \partial_x \boldsymbol{Z}_{ij} = \nabla_{\boldsymbol{z}} S(\boldsymbol{Z}_{ij}), \ \ 1 \le i \le r, \ 1 \le j \le s, \ 1 \le \gamma \le \alpha, \end{aligned} \tag{2.5}$$

where $\boldsymbol{Z}_{ij}^{(\gamma)} \approx \boldsymbol{z}(t_0 + c_i^{(\gamma)} \Delta t, x_0 + \widetilde{c}_j^{(\gamma)} \Delta x)$, $\boldsymbol{z}_j^{(\gamma)0} \approx \boldsymbol{z}(t_0, x_0 + \widetilde{c}_j^{(\gamma)} \Delta x)$, $\boldsymbol{z}_j^{(\gamma)1} \approx \boldsymbol{z}(t_0 + \Delta t, x_0 + \widetilde{c}_j^{(\gamma)} \Delta x)$, $\boldsymbol{z}_0^{(\gamma)i} \approx \boldsymbol{z}(t_0 + c_i^{(\gamma)} \Delta t, x_0)$, $\boldsymbol{z}_1^{(\gamma)i} \approx \boldsymbol{z}(t_0 + c_i^{(\gamma)} \Delta t, x_0 + \Delta x)$.

It is shown that the above discretization is called multi-symplecticity if its PRK coefficients satisfy some conditions [12, 23]. However, it should be careful to implement the numerical discretization of high order as it may fail to be well-defined [23,18]. In fact, the above numerical discretization may involve the computation of a differential-algebraic system. In this paper, we will be concerned with the DG approach for solving Hamiltonian differential equations, and we will see that the resulting algorithms, under certain requirements on the differential equations, are well-defined and can be related to PRK schemes. The benefit of the DG approach in our design for multi-symplectic algorithms is that we get ODEs other than differential-algebraic systems which naturally avoids considering the solvability of a differential-algebraic system.

3. DG methods for Hamiltonian ODEs

The Hamiltonian system is written in the form

$$\boldsymbol{p}_t = -\nabla_{\boldsymbol{q}} \mathbf{H}(\boldsymbol{p}, \boldsymbol{q}), \ \boldsymbol{q}_t = \nabla_{\boldsymbol{p}} \mathbf{H}(\boldsymbol{p}, \boldsymbol{q}), \quad t \in I = [t_0, T], \tag{3.1}$$

with the initial values $\boldsymbol{p}(t_0) = \boldsymbol{p}_0$, $\boldsymbol{q}(t_0) = \boldsymbol{q}_0$. Here, $\boldsymbol{p}$ denotes the momenta and $\boldsymbol{q}$ denotes the position, the Hamiltonian (namely the total energy) $\mathbf{H}(\boldsymbol{p}, \boldsymbol{q})$ is assumed to be smooth. It is known that the exact flow φ_t of system (3.1) is symplectic [10], namely φ_t satisfies $(\varphi_t')^T J \varphi_t' = J$, where J is a canonical structure matrix and φ_t' denotes the Jacobian matrix of φ_t. A one-step method $\Phi_h : (\boldsymbol{p}_n, \boldsymbol{q}_n) \mapsto (\boldsymbol{p}_{n+1}, \boldsymbol{q}_{n+1})$ applied to the Hamiltonian system (3.1) is called symplectic if and only if $(\Phi_h')^T J \Phi_h' = J$.

By dividing the time interval I as $I = \bigcup_{j=0}^{N-1}[t_j, t_{j+1}] = \bigcup_{j=0}^{N-1} I_j$ and defining the finite element space $V_{\Delta t}^k(I) = \{\chi : \chi|_{I_j} \in (\mathbb{P}^k(I_j))^d,\ 0 \le j \le N-1\}$ with $\Delta t_j \equiv \Delta t$, the DG method applied to (3.1) reads

$$\begin{aligned} &\int_{I_j} (\boldsymbol{P}\cdot\phi_t - \nabla_{\boldsymbol{q}}\mathbf{H}(\boldsymbol{P},\boldsymbol{Q})\cdot\phi)\,\mathrm{d}t - \widehat{\boldsymbol{P}}_{j+1}\cdot\phi_{j+1}^- + \widehat{\boldsymbol{P}}_j\cdot\phi_j^+ = 0,\\ &\int_{I_j} (\boldsymbol{Q}\cdot\psi_t + \nabla_{\boldsymbol{p}}\mathbf{H}(\boldsymbol{P},\boldsymbol{Q})\cdot\psi)\,\mathrm{d}t - \widehat{\boldsymbol{Q}}_{j+1}\cdot\psi_{j+1}^- + \widehat{\boldsymbol{Q}}_j\cdot\psi_j^+ = 0, \end{aligned} \tag{3.2}$$

where $\phi,\ \psi \in V_{\Delta t}^k(I),\ 0 \le j \le N-1$.

To make the numerical solutions of DG algorithm (3.2) well defined, we need carefully choose the numerical fluxes. We choose the numerical fluxes as

$$\widehat{\boldsymbol{P}} = \boldsymbol{P}^-,\ \ \widehat{\boldsymbol{Q}} = \boldsymbol{Q}^+, \tag{3.3}$$

or

$$\widehat{\boldsymbol{P}} = \boldsymbol{P}^+,\ \ \widehat{\boldsymbol{Q}} = \boldsymbol{Q}^-. \tag{3.4}$$

As above, we have omitted the indices j. If the DG polynomial is a polynomial of degree $k = 0$, then the DG method with the fluxes (3.3) or (3.4) provides the well-known symplectic Euler method, which was the first symplectic method proposed in 1956 by de Vogelaere [8,10]. Assume that the DG approximation is a polynomial of k-degree, then it can be expressed as

$$\boldsymbol{P}(t) = \sum_{\iota=1}^{k+1} \boldsymbol{P}_\iota^j \varphi_\iota(t),\ \ \boldsymbol{Q}(t) = \sum_{\iota=1}^{k+1} \boldsymbol{Q}_\iota^j \varphi_\iota(t), \qquad t \in I_j \tag{3.5}$$

with $\boldsymbol{Q}_\iota^j, \boldsymbol{P}_\iota^j$ the unknown coefficients and φ_ι the local basis functions.

As follows, we show that scheme (3.2) can be connected to a symplectic PRK scheme. In order to show this, we introduce the ι-degree normalized shifted Legendre orthogonal polynomials by

$$\rho_\iota(x) = \frac{\sqrt{2\iota+1}}{\iota!}\frac{d^\iota}{dx^\iota}\left(x^\iota(x-1)^\iota\right),\ \ \iota = 0, 1, 2, \cdots. \tag{3.6}$$

We claim that the DG scheme (3.2) defined on I_j with flux (3.3) is equivalent to the following continuous-stage PRK method[1] with $\tau \in [0,1]$ (see Appendix for more details)

$$\begin{aligned} &\boldsymbol{P}_\tau = \widehat{\boldsymbol{P}}_j + \Delta t\int_0^1 A_{\tau,\sigma}^{(1)}\boldsymbol{f}(\boldsymbol{P}_\sigma,\boldsymbol{Q}_\sigma)\,\mathrm{d}\sigma,\ \ \boldsymbol{Q}_\tau = \widehat{\boldsymbol{Q}}_j + \Delta t\int_0^1 A_{\tau,\sigma}^{(2)}\boldsymbol{g}(\boldsymbol{P}_\sigma,\boldsymbol{Q}_\sigma)\,\mathrm{d}\sigma,\\ &\widehat{\boldsymbol{P}}_{j+1} = \widehat{\boldsymbol{P}}_j + \Delta t\int_0^1 \boldsymbol{f}(\boldsymbol{P}_\tau,\boldsymbol{Q}_\tau)\,\mathrm{d}\tau,\ \ \widehat{\boldsymbol{Q}}_{j+1} = \widehat{\boldsymbol{Q}}_j + \Delta t\int_0^1 \boldsymbol{g}(\boldsymbol{P}_\tau,\boldsymbol{Q}_\tau)\,\mathrm{d}\tau, \end{aligned} \tag{3.7}$$

where $\boldsymbol{P}_\tau = \boldsymbol{P}(t_j + \tau\Delta t),\ \boldsymbol{Q}_\tau = \boldsymbol{Q}(t_j + \tau\Delta t),\ \boldsymbol{f}(\boldsymbol{p},\boldsymbol{q}) = -\nabla_{\boldsymbol{q}}\mathbf{H}(\boldsymbol{p},\boldsymbol{q}),\ \boldsymbol{g}(\boldsymbol{p},\boldsymbol{q}) = \nabla_{\boldsymbol{p}}\mathbf{H}(\boldsymbol{p},\boldsymbol{q})$. In (3.7), the PRK coefficients are defined as

$$\begin{aligned} A_{\tau,\sigma}^{(1)} &= 1 + \frac{1}{\sqrt{2k+1}}\sum_{\iota=0}^{k-1}\left(\sqrt{2\iota+1}\rho_k(\tau) - \sqrt{2k+1}\rho_\iota(\tau)\right)\int_0^\sigma \rho_\iota(x)\,\mathrm{d}x,\\ A_{\tau,\sigma}^{(2)} &= \frac{1}{\sqrt{2k+1}}\sum_{\iota=0}^{k-1}\left(\sqrt{2k+1}\rho_\iota(\sigma) - \sqrt{2\iota+1}\rho_k(\sigma)\right)\int_0^\tau \rho_\iota(x)\,\mathrm{d}x. \end{aligned} \tag{3.8}$$

If we choose flux (3.4), then the PRK coefficients are changed to

[1] Continuous-stage (partitioned) Runge–Kutta method is a class of infinitely many stage (P)RK-type methods discussed in [11,28,29,31,30].

$$A^{(1)}_{\tau,\sigma} = \frac{1}{\sqrt{2k+1}} \sum_{\iota=0}^{k-1} \left(\sqrt{2k+1}\rho_\iota(\sigma) - \sqrt{2\iota+1}\rho_k(\sigma) \right) \int_0^\tau \rho_\iota(x)\,\mathrm{d}x,$$
$$A^{(2)}_{\tau,\sigma} = 1 + \frac{1}{\sqrt{2k+1}} \sum_{\iota=0}^{k-1} \left(\sqrt{2\iota+1}\rho_k(\tau) - \sqrt{2k+1}\rho_\iota(\tau) \right) \int_0^\sigma \rho_\iota(x)\,\mathrm{d}x. \tag{3.9}$$

Applying a quadrature formula $(b_n, c_n)_{n=1}^s$ to (3.7), gives the following s-stage PRK scheme

$$\boldsymbol{P}_{c_n} = \widehat{\boldsymbol{P}}_j + \Delta t \sum_{\iota=1}^s a^{(1)}_{n\iota} \boldsymbol{f}(\boldsymbol{P}_{c_\iota}, \boldsymbol{Q}_{c_\iota}),\ \boldsymbol{Q}_{c_n} = \widehat{\boldsymbol{Q}}_j + \Delta t \sum_{\iota=1}^s a^{(2)}_{n\iota} \boldsymbol{g}(\boldsymbol{P}_{c_\iota}, \boldsymbol{Q}_{c_\iota}),$$
$$\widehat{\boldsymbol{P}}_{j+1} = \widehat{\boldsymbol{P}}_j + \Delta t \sum_{n=1}^s b^{(1)}_n \boldsymbol{f}(\boldsymbol{P}_{c_n}, \boldsymbol{Q}_{c_n}),\ \widehat{\boldsymbol{Q}}_{j+1} = \widehat{\boldsymbol{Q}}_j + \Delta t \sum_{n=1}^s b^{(2)}_n \boldsymbol{g}(\boldsymbol{P}_{c_n}, \boldsymbol{Q}_{c_n}),$$

with $n = 1, \cdots, s$, where $a^{(1)}_{n\iota} = b_\iota A^{(1)}_{c_n, c_\iota}$, $b^{(1)}_n = b_n$ and $a^{(2)}_{n\iota} = b_\iota A^{(2)}_{c_n, c_\iota}$, $b^{(2)}_n = b_n$. Note that applying a quadrature formula to (3.7) is equivalent applying the same quadrature formula to the nonlinear terms of (3.2) (namely the terms involving the Hamiltonian). Now we give the main results of this section.

Theorem 3.1. *The DG method (3.2) with fluxes (3.3) or (3.4) for solving Hamiltonian system (3.1) is equivalent to a symplectic continuous-stage PRK method with a superconvergence order $2k+1$. Moreover, if we use a quadrature formula $(b_n, c_n)_{n=1}^s$ of order [2] p to calculate the nonlinear term, then the resulting scheme is equivalent to an s-stage symplectic PRK scheme of order* $\min(p, 2k+1, 2p-2k+1)$.

Proof. From (3.8) or (3.9) we have $A^{(1)}_{c_n,c_\iota} + A^{(2)}_{c_\iota,c_n} = 1$ for $n, \iota = 1, \cdots, s$. Then, it is easy to get $b_n b_\iota A^{(1)}_{c_n,c_\iota} + b_\iota b_n A^{(2)}_{c_\iota,c_n} = b_n b_\iota$, $n, \iota = 1, \cdots, s$. Denote $a^{(1)}_{n\iota} = b_\iota A^{(1)}_{c_n,c_\iota}$, $b^{(1)}_n = b_n$, $a^{(2)}_{n\iota} = b_\iota A^{(2)}_{c_n,c_\iota}$ and $b^{(2)}_n = b_n$, this implies $b^{(1)}_n a^{(2)}_{n\iota} + b^{(2)}_\iota a^{(1)}_{\iota n} - b^{(1)}_n b^{(2)}_\iota = 0, n, \iota = 1, \cdots, s$ and thus the scheme is symplectic by a classical result (see Theorem 4.6 [10], p. 193). The order of the scheme can be directly verified by Theorem 2.3 and 2.5 in [30]. □

Remark 3.1. The time finite element method (TFEM) constructed by combining k-degree left-discontinuous and right-discontinuous TFEMs in [29] can be retrieved from the DG scheme (3.2).

Remark 3.2. By using different quadrature formulae, we can get different symplectic PRK schemes from the DG method. They can cover most of the high-order symplectic (P)RK schemes in literature (see, e.g. [26]), such as Gauss–Legendre RK scheme, Gauss IA-IĀ, Radau IA-IĀ, Radau IIA-IIĀ and Lobatto IIIC-IIIC̄ PRK schemes, etc. [29].

4. DG methods for Hamiltonian PDEs

In this section, we extend the results presented in the previous section to the case of Hamiltonian PDEs. As it was introduced in [4] that many conservative PDEs can be written in the following form

$$M\boldsymbol{z}_t + K\boldsymbol{z}_x = \nabla_{\boldsymbol{z}} S(\boldsymbol{z}), \tag{4.1}$$

where $\boldsymbol{z} \in \mathbb{R}^d$, M, K are two skew-symmetric matrices in $\mathbb{R}^{d\times d}$, and $S(\boldsymbol{z})$ is a smooth scalar function.

The system (4.1) is called multi-symplectic as it has the multi-symplectic structure [22]

$$\partial_t(\mathrm{d}\boldsymbol{z} \wedge M\mathrm{d}\boldsymbol{z}) + \partial_x(\mathrm{d}\boldsymbol{z} \wedge K\mathrm{d}\boldsymbol{z}) = 0, \tag{4.2}$$

where $\wedge$ denotes the exterior product. Besides this structure, it is also known to have two local conservation laws [22]:

(1) $\partial_t \left(S(\boldsymbol{z}) - \frac{1}{2}\boldsymbol{z}^T K \boldsymbol{z}_x \right) + \partial_x \left(\frac{1}{2}\boldsymbol{z}^T K \boldsymbol{z}_t \right) = 0$ (energy conservation);
(2) $\partial_t \left(\frac{1}{2}\boldsymbol{z}^T M \boldsymbol{z}_x \right) + \partial_x \left(S(\boldsymbol{z}) - \frac{1}{2}\boldsymbol{z}^T M \boldsymbol{z}_t \right) = 0$ (momentum conservation).

A numerical method which preserves a discrete version of the multi-symplectic conservation law (4.2) is referred to as a multi-symplectic numerical method [4,19]. Usually, such kind of algorithms have remarkable energy and momentum

[2] This means that the formula $\int_0^1 f(x)\,\mathrm{d}x = \sum_{n=1}^s b_n f(c_n)$ exactly holds for any polynomials of degree up to $p-1$.

conservative properties (see [13,27] and the references therein). Besides, energy preserving and momentum preserving algorithms are also of interest and they belong to the class of conservative numerical methods.

Assume d is even, then the Hamiltonian PDEs (4.1) can be written in the following partitioned form

$$\begin{pmatrix} M_{11} & M_{12} \\ M_{21} & M_{22} \end{pmatrix} \begin{pmatrix} \boldsymbol{p} \\ \boldsymbol{q} \end{pmatrix}_t + \begin{pmatrix} K_{11} & K_{12} \\ K_{21} & K_{22} \end{pmatrix} \begin{pmatrix} \boldsymbol{p} \\ \boldsymbol{q} \end{pmatrix}_x = \begin{pmatrix} \nabla_{\boldsymbol{p}} S(\boldsymbol{p}, \boldsymbol{q}) \\ \nabla_{\boldsymbol{q}} S(\boldsymbol{p}, \boldsymbol{q}) \end{pmatrix}, \tag{4.3}$$

where $\boldsymbol{p}$ and $\boldsymbol{q}$ are two $d/2$-dimensional vector functions, M_{11} and M_{22} are two skew-symmetric matrices, and $M_{12}^T = -M_{21}$. We also assume that one of the following conditions is fulfilled:

(a) $K_{11} \equiv \mathbf{0}$, $K_{22} \equiv \mathbf{0}$, $K_{12}^T = -K_{21} \neq \mathbf{0}$;
(b) $K_{11} \neq \mathbf{0}$, $K_{22} \neq \mathbf{0}$, $K_{12}^T = -K_{21} \equiv \mathbf{0}$.

Since the discussions for both cases are very similar, we take case (a) as an illustration. Now we apply the DG approach to discretize (4.3) in space, then it gives the following variational formulation

$$\begin{aligned} &\int_{\Omega_j} (\nabla_{\boldsymbol{p}} S(\boldsymbol{P}, \boldsymbol{Q}) - M_{11}\boldsymbol{P}_t - M_{12}\boldsymbol{Q}_t)\phi \mathrm{d}x + K_{12}\left(\int_{\Omega_j} \boldsymbol{Q}\phi_x \mathrm{d}x - \widehat{\boldsymbol{Q}}_{j+1}\phi_{j+1}^- + \widehat{\boldsymbol{Q}}_j \phi_j^+ \right) = 0, \\ &\int_{\Omega_j} (\nabla_{\boldsymbol{q}} S(\boldsymbol{P}, \boldsymbol{Q}) - M_{21}\boldsymbol{P}_t - M_{22}\boldsymbol{Q}_t)\psi \mathrm{d}x + K_{21}\left(\int_{\Omega_j} \boldsymbol{P}\psi_x \mathrm{d}x - \widehat{\boldsymbol{P}}_{j+1}\psi_{j+1}^- + \widehat{\boldsymbol{P}}_j \psi_j^+ \right) = 0, \end{aligned} \tag{4.4}$$

where $\boldsymbol{P}(\cdot, x), \boldsymbol{Q}(\cdot, x), \phi, \psi \in V_{\Delta x}^k(\Omega)$ and $j = 0, \cdots, N-1$. To proceed our discussions, we assume that both K_{12} and K_{21} are non-singular (though this is not very necessary), and we introduce the following notations

$$\begin{aligned} \boldsymbol{f}(\boldsymbol{p}, \boldsymbol{q}, \boldsymbol{p}_t, \boldsymbol{q}_t) &= K_{12}^{-1}(\nabla_{\boldsymbol{p}} S(\boldsymbol{p}, \boldsymbol{q}) - M_{11}\boldsymbol{p}_t - M_{12}\boldsymbol{q}_t), \\ \boldsymbol{g}(\boldsymbol{p}, \boldsymbol{q}, \boldsymbol{p}_t, \boldsymbol{q}_t) &= K_{21}^{-1}(\nabla_{\boldsymbol{q}} S(\boldsymbol{p}, \boldsymbol{q}) - M_{21}\boldsymbol{p}_t - M_{22}\boldsymbol{q}_t). \end{aligned}$$

Then formally, (4.3) leads to an ODEs in space

$$\boldsymbol{q}_x = \boldsymbol{f}(\boldsymbol{p}, \boldsymbol{q}, \boldsymbol{p}_t, \boldsymbol{q}_t), \ \boldsymbol{p}_x = \boldsymbol{g}(\boldsymbol{p}, \boldsymbol{q}, \boldsymbol{p}_t, \boldsymbol{q}_t). \tag{4.5}$$

In such a case, we can rewrite (4.4) as

$$\begin{aligned} &\int_{\Omega_j} \boldsymbol{f}(\boldsymbol{P}, \boldsymbol{Q}, \boldsymbol{P}_t, \boldsymbol{Q}_t)\phi \mathrm{d}x + \int_{\Omega_j} \boldsymbol{Q}\phi_x \mathrm{d}x - \widehat{\boldsymbol{Q}}_{j+1}\phi_{j+1}^- + \widehat{\boldsymbol{Q}}_j \phi_j^+ = 0, \\ &\int_{\Omega_j} \boldsymbol{g}(\boldsymbol{P}, \boldsymbol{Q}, \boldsymbol{P}_t, \boldsymbol{Q}_t)\psi \mathrm{d}x + \int_{\Omega_j} \boldsymbol{P}\psi_x \mathrm{d}x - \widehat{\boldsymbol{P}}_{j+1}\psi_{j+1}^- + \widehat{\boldsymbol{P}}_j \psi_j^+ = 0. \end{aligned} \tag{4.6}$$

Now we choose the numerical fluxes as $\widehat{\boldsymbol{Q}} = \boldsymbol{Q}^-$, $\widehat{\boldsymbol{P}} = \boldsymbol{P}^+$ (resp. $\widehat{\boldsymbol{Q}} = \boldsymbol{Q}^+$, $\widehat{\boldsymbol{P}} = \boldsymbol{P}^-$), then the DG scheme (4.6) can be reshaped as

$$\begin{aligned} \boldsymbol{Q}_\tau &= \widehat{\boldsymbol{Q}}_j + \Delta x_j \int_0^1 A_{\tau,\sigma}^{(1)} \boldsymbol{f}(\boldsymbol{P}_\sigma, \boldsymbol{Q}_\sigma, (\boldsymbol{P}_\sigma)_t, (\boldsymbol{Q}_\sigma)_t) \mathrm{d}\sigma, \quad \tau \in [0, 1], \\ \boldsymbol{P}_\tau &= \widehat{\boldsymbol{P}}_j + \Delta x_j \int_0^1 A_{\tau,\sigma}^{(2)} \boldsymbol{g}(\boldsymbol{P}_\sigma, \boldsymbol{Q}_\sigma, (\boldsymbol{P}_\sigma)_t, (\boldsymbol{Q}_\sigma)_t) \mathrm{d}\sigma, \quad \tau \in [0, 1], \\ \widehat{\boldsymbol{Q}}_{j+1} &= \widehat{\boldsymbol{Q}}_j + \Delta x_j \int_0^1 \boldsymbol{f}(\boldsymbol{P}_\tau, \boldsymbol{Q}_\tau, (\boldsymbol{P}_\tau)_t, (\boldsymbol{Q}_\tau)_t) \mathrm{d}\tau, \\ \widehat{\boldsymbol{P}}_{j+1} &= \widehat{\boldsymbol{P}}_j + \Delta x_j \int_0^1 \boldsymbol{g}(\boldsymbol{P}_\tau, \boldsymbol{Q}_\tau, (\boldsymbol{P}_\tau)_t, (\boldsymbol{Q}_\tau)_t) \mathrm{d}\tau, \end{aligned} \tag{4.7}$$

which is obtained by the same process as made in Appendix, where $\mathbf{\Phi}_\tau := \mathbf{\Phi}(\cdot, x_j + \tau\Delta x_j)$, and $A^{(1)}_{\tau,\sigma}, A^{(2)}_{\tau,\sigma}$ are given by (3.8) (resp. (3.9)). Assume that the spatial step is uniform which is denoted by $\Delta x_j \equiv \Delta x,\ j = 0, \cdots, N-1$, then applying a quadrature formula denoted by $(b_n, c_n)_{n=1}^s$ to (4.7) gives

$$\begin{aligned}
&\boldsymbol{Q}_{c_n} = \widehat{\boldsymbol{Q}}_j + \Delta x \sum_{\iota=1}^{s} a^{(1)}_{n\iota} \overline{\boldsymbol{Q}}_x(\cdot, x_j + c_\iota \Delta x), \qquad n = 1, \cdots, s,\\
&\boldsymbol{P}_{c_n} = \widehat{\boldsymbol{P}}_j + \Delta x \sum_{\iota=1}^{s} a^{(2)}_{n\iota} \overline{\boldsymbol{P}}_x(\cdot, x_j + c_\iota \Delta x), \qquad n = 1, \cdots, s,\\
&\widehat{\boldsymbol{Q}}_{j+1} = \widehat{\boldsymbol{Q}}_j + \Delta x \sum_{n=1}^{s} b^{(1)}_n \overline{\boldsymbol{Q}}_x(\cdot, x_j + c_n \Delta x),\\
&\widehat{\boldsymbol{P}}_{j+1} = \widehat{\boldsymbol{P}}_j + \Delta x \sum_{n=1}^{s} b^{(2)}_n \overline{\boldsymbol{P}}_x(\cdot, x_j + c_n \Delta x)
\end{aligned} \tag{4.8}$$

with $a^{(1)}_{n\iota} = b_\iota A^{(1)}_{c_n, c_\iota}$, $b^{(1)}_n = b_n$, $a^{(2)}_{n\iota} = b_\iota A^{(2)}_{c_n, c_\iota}$, $b^{(2)}_n = b_n$, $n, \iota = 1, \cdots, s$. In (4.8), we have used the following notations

$$\begin{aligned}
&\overline{\boldsymbol{Q}}_x(\cdot, x_j + c_\iota \Delta x_j) = \boldsymbol{f}(\boldsymbol{P}_{c_\iota}, \boldsymbol{Q}_{c_\iota}, (\boldsymbol{P}_{c_\iota})_t, (\boldsymbol{Q}_{c_\iota})_t), \quad \iota = 1, \cdots, s,\\
&\overline{\boldsymbol{P}}_x(\cdot, x_j + c_\iota \Delta x_j) = \boldsymbol{g}(\boldsymbol{P}_{c_\iota}, \boldsymbol{Q}_{c_\iota}, (\boldsymbol{P}_{c_\iota})_t, (\boldsymbol{Q}_{c_\iota})_t), \quad \iota = 1, \cdots, s,
\end{aligned} \tag{4.9}$$

which can be taken as a collocation-like discretization associated with Eqs. (4.5).

Remark 4.1. If the sub-block matrices K_{12} and K_{21} in (4.3) are singular (but non-zero), then the ODEs (4.5) can be rewritten as

$$K_{12}\boldsymbol{q}_x = \boldsymbol{f}(\boldsymbol{p}, \boldsymbol{q}, \boldsymbol{p}_t, \boldsymbol{q}_t),\ K_{21}\boldsymbol{p}_x = \boldsymbol{g}(\boldsymbol{p}, \boldsymbol{q}, \boldsymbol{p}_t, \boldsymbol{q}_t),$$

with $\boldsymbol{f}(\boldsymbol{p}, \boldsymbol{q}, \boldsymbol{p}_t, \boldsymbol{q}_t) = \nabla_{\boldsymbol{p}} S(\boldsymbol{p}, \boldsymbol{q}) - M_{11}\boldsymbol{p}_t - M_{12}\boldsymbol{q}_t$ and $\boldsymbol{g}(\boldsymbol{p}, \boldsymbol{q}, \boldsymbol{p}_t, \boldsymbol{q}_t) = \nabla_{\boldsymbol{q}} S(\boldsymbol{p}, \boldsymbol{q}) - M_{21}\boldsymbol{p}_t - M_{22}\boldsymbol{q}_t$. In such a case, we can still obtain a continuous-stage PRK scheme which is similar to (4.7) (only need to multiply K_{12} and K_{21} from the left-hand side). There will be no influence on getting multi-symplectic integrators.

Now we use an r-stage PRK method with coefficients $(A^{(\gamma)}_{n\iota}, B^{(\gamma)}_n, d_n)(1 \le \gamma \le 2)$ to discretize the semi-discretized system (4.8) in time, then it gives rise to

$$\boldsymbol{Q}_{mn} = q^m_0 + \Delta x \sum_{\iota=1}^{s} a^{(1)}_{n\iota} \partial_x \boldsymbol{Q}_{m\iota}, \qquad \boldsymbol{P}_{mn} = p^m_0 + \Delta x \sum_{\iota=1}^{s} a^{(2)}_{n\iota} \partial_x \boldsymbol{P}_{m\iota}, \tag{4.10}$$

$$q^m_1 = q^m_0 + \Delta x \sum_{\iota=1}^{s} b^{(1)}_\iota \partial_x \boldsymbol{Q}_{m\iota}, \qquad p^m_1 = p^m_0 + \Delta x \sum_{\iota=1}^{s} b^{(2)}_\iota \partial_x \boldsymbol{P}_{m\iota}, \tag{4.11}$$

$$\boldsymbol{Q}_{mn} = q^0_n + \Delta t \sum_{\iota=1}^{r} A^{(1)}_{m\iota} \partial_t \boldsymbol{Q}_{\iota n}, \qquad \boldsymbol{P}_{mn} = p^0_n + \Delta t \sum_{\iota=1}^{r} A^{(2)}_{m\iota} \partial_t \boldsymbol{P}_{\iota n}, \tag{4.12}$$

$$q^1_n = q^0_n + \Delta t \sum_{\iota=1}^{r} B^{(1)}_\iota \partial_t \boldsymbol{Q}_{\iota n}, \qquad p^1_n = p^0_n + \Delta t \sum_{\iota=1}^{r} B^{(2)}_\iota \partial_t \boldsymbol{P}_{\iota n}, \tag{4.13}$$

where

$$\begin{aligned}
q^m_0 &\approx \widehat{\boldsymbol{Q}}_0(t_0 + d_m\Delta t), & q^m_1 &\approx \widehat{\boldsymbol{Q}}_1(t_0 + d_m\Delta t),\\
p^m_0 &\approx \widehat{\boldsymbol{P}}_0(t_0 + d_m\Delta t), & p^m_1 &\approx \widehat{\boldsymbol{P}}_1(t_0 + d_m\Delta t),\\
q^0_n &\approx \boldsymbol{Q}(t_0, x_0 + c_n\Delta x), & q^1_n &\approx \boldsymbol{Q}(t_0 + \Delta t, x_0 + c_n\Delta x),\\
p^0_n &\approx \boldsymbol{P}(t_0, x_0 + c_n\Delta x), & p^1_n &\approx \boldsymbol{P}(t_0 + \Delta t, x_0 + c_n\Delta x),\\
\boldsymbol{Q}_{mn} &\approx \boldsymbol{Q}(t_0 + d_m\Delta t, x_0 + c_n\Delta x), & \boldsymbol{P}_{mn} &\approx \boldsymbol{P}(t_0 + d_m\Delta t, x_0 + c_n\Delta x),\\
\partial_x \boldsymbol{Q}_{mn} &\approx \overline{\boldsymbol{Q}}_x(t_0 + d_m\Delta t, x_0 + c_n\Delta x), & \partial_x \boldsymbol{P}_{mn} &\approx \overline{\boldsymbol{P}}_x(t_0 + d_m\Delta t, x_0 + c_n\Delta x),\\
\partial_t \boldsymbol{Q}_{mn} &\approx \boldsymbol{Q}_t(t_0 + d_m\Delta t, x_0 + c_n\Delta x), & \partial_t \boldsymbol{P}_{mn} &\approx \boldsymbol{P}_t(t_0 + d_m\Delta t, x_0 + c_n\Delta x).
\end{aligned}$$

In the above equalities, $\boldsymbol{P}_{mn}, \boldsymbol{Q}_{mn}, \partial_t \boldsymbol{P}_{mn}, \partial_t \boldsymbol{Q}_{mn}, \partial_x \boldsymbol{P}_{mn}, \partial_x \boldsymbol{Q}_{mn}$ satisfy

$$\begin{pmatrix} M_{11} & M_{12} \\ M_{21} & M_{22} \end{pmatrix} \begin{pmatrix} \partial_t \boldsymbol{P}_{mn} \\ \partial_t \boldsymbol{Q}_{mn} \end{pmatrix} + \begin{pmatrix} \boldsymbol{0} & K_{12} \\ K_{21} & \boldsymbol{0} \end{pmatrix} \begin{pmatrix} \partial_x \boldsymbol{P}_{mn} \\ \partial_x \boldsymbol{Q}_{mn} \end{pmatrix} = \begin{pmatrix} \nabla_{\boldsymbol{p}} S(\boldsymbol{P}_{mn}, \boldsymbol{Q}_{mn}) \\ \nabla_{\boldsymbol{q}} S(\boldsymbol{P}_{mn}, \boldsymbol{Q}_{mn}) \end{pmatrix} \tag{4.14}$$

with $m = 1, \cdots, r$, $n = 1, \cdots, s$. Combining the DG discretization in space and PRK discretization in time we get a full discretization which is equivalent to a time-space PRK scheme.

Lemma 4.1. *[23] For the discretization of multi-symplectic Hamiltonian PDEs (4.1), if we employ an r-stage PRK method with coefficients $(A_{n\iota}^{(\gamma)}, B_n^{(\gamma)}, d_n)$ in the time direction and an s-stage PRK method with coefficients $(a_{n\iota}^{(\gamma)}, b_n^{(\gamma)}, c_n)$ in the space direction, then the resulting full discretization is multi-symplectic if the following conditions hold:*

$$\begin{aligned} &B_n^{(\alpha)} = B_n, \qquad n = 1, \cdots, r, \\ &B_n^{(\alpha)} A_{n\iota}^{(\beta)} + B_\iota^{(\beta)} A_{\iota n}^{(\alpha)} - B_n^{(\alpha)} B_\iota^{(\beta)} = 0, \qquad n, \iota = 1, \cdots, r \end{aligned} \tag{4.15}$$

for all the pairs (α, β) such that $M_{\alpha\beta} \neq \boldsymbol{0}$ and

$$\begin{aligned} &b_n^{(\alpha)} = b_n, \qquad n = 1, \cdots, s, \\ &b_n^{(\alpha)} a_{n\iota}^{(\beta)} + b_\iota^{(\beta)} a_{\iota n}^{(\alpha)} - b_n^{(\alpha)} b_\iota^{(\beta)} = 0, \qquad n, \iota = 1, \cdots, s \end{aligned} \tag{4.16}$$

for all the pairs (α, β) such that $K_{\alpha\beta} \neq \boldsymbol{0}$.

From the above lemma, we address the following theorem.

Theorem 4.1. *With a quadrature formula and a suitable symplectic (P)RK method for the time integration, from the DG scheme (4.4) we can get a multi-symplectic scheme which is equivalent to a time-space PRK scheme.*

Proof. Assume that the variables $\boldsymbol{z}$ are partitioned into two parts both in space and time for PRK discretizations. It is known that the conditions in (4.16) are automatically satisfied by the DG discretization in space (see Theorem 3.1). Therefore, if we use a suitable symplectic (P)RK discretization for the time integration (namely its PRK coefficients satisfying (4.15)), then we get a multi-symplectic PRK scheme by Lemma 4.1. □

Next, let us proceed to consider the more general case. Assume a multi-symplectic Hamiltonian PDEs is in a partitioned form

$$M\boldsymbol{z}_t + \begin{pmatrix} K_{11} & \cdots & K_{1\alpha} \\ \vdots & \ldots & \vdots \\ K_{\alpha 1} & \cdots & K_{\alpha\alpha} \end{pmatrix} \begin{pmatrix} \boldsymbol{z}^{(1)} \\ \vdots \\ \boldsymbol{z}^{(\alpha)} \end{pmatrix}_x = \begin{pmatrix} \nabla_{\boldsymbol{z}^{(1)}} S(\boldsymbol{z}) \\ \vdots \\ \nabla_{\boldsymbol{z}^{(\alpha)}} S(\boldsymbol{z}) \end{pmatrix}, \tag{4.17}$$

where $\boldsymbol{z}(t, x) \in \mathbb{R}^d$ is decomposed into α parts. Now we assume that the block matrix K in (4.17) has the following *structure features*: there is an index chain denoted by $1 \leq i_1 < \cdots < i_m \leq \alpha$ with $m \leq \alpha$ and an index set $\{j_1, \cdots, j_m\} \subseteq \{1, 2, \cdots, \alpha\}$ such that $K_{i_1 j_1}, \cdots, K_{i_m j_m}$ are non-zero matrices, and all the other sub-block matrices of K are zero. In such a case, by performing the similar discussions as above, the DG approach can be used to discretize the variables $\boldsymbol{z}_x^{(i_s)}$ and $\boldsymbol{z}_x^{(j_s)}$ $(s = 1, \cdots, m)$ in space. For the purpose of deriving a multi-symplectic scheme, the fluxes $\widehat{\boldsymbol{z}^{(i_s)}}$ and $\widehat{\boldsymbol{z}^{(j_s)}}$ must be taken from different directions for each given s. This holds true because when we use DG discretization in space for each pair $(\boldsymbol{z}_x^{(i_s)}, \boldsymbol{z}_x^{(j_s)})$, the PRK coefficients automatically satisfy (4.16) and it will not influence other pairs.

Remark 4.2. For a skew-symmetric matrix $K \in \mathbb{R}^{d\times d}$, there exists a real orthogonal U such that (see [14], p. 136)

$$U^T K U = \mathrm{diag}(0, \cdots, 0, \Lambda_1, \cdots, \Lambda_s) \in \mathbb{R}^{d\times d}, \quad 2s \leq d,$$

where $\Lambda_i = \begin{pmatrix} 0 & \lambda_i \\ -\lambda_i & 0 \end{pmatrix}$, $\lambda_i \in \mathbb{R}^+$, $i = 1, \cdots, s$. Therefore, by introducing a new variable $\widetilde{\boldsymbol{z}} = U^{-1}\boldsymbol{z}$ we can always reform a given system (4.1) into a new system in the form (4.17) with the structure described as above.

Remark 4.3. For Hamiltonian PDEs (4.1), in this paper we only consider the DG discretization in space. This can be generalized to consider the numerical discretizations derived by the DG method both in space and time.

In what follows, we give some examples to show how to choose the appropriate numerical fluxes for the sake of constructing multi-symplectic integrators.

Example 4.1. Consider the nonlinear Klein–Gordon equation

$$u_{tt} = u_{xx} - F'(u), \ \ (t,x) \in \mathbb{R}^2, \tag{4.18}$$

where $F : \mathbb{R} \longmapsto \mathbb{R}$ is a scalar function. Let $v = u_t$, $w = u_x$, then (4.18) can be recast as [22]

$$M\boldsymbol{z}_t + K\boldsymbol{z}_x = \nabla_{\boldsymbol{z}} S(\boldsymbol{z}),$$

where

$$M = \begin{pmatrix} 0 & -1 & 0 \\ 1 & 0 & 0 \\ 0 & 0 & 0 \end{pmatrix}, \ K = \begin{pmatrix} 0 & 0 & 1 \\ 0 & 0 & 0 \\ -1 & 0 & 0 \end{pmatrix}, \ \boldsymbol{z} = \begin{pmatrix} u \\ v \\ w \end{pmatrix},$$

and $S(\boldsymbol{z}) = \frac{1}{2}(v^2 - w^2) + F(u)$.

Applying the DG method to semi-discretize the above multi-symplectic system, then we get the following variational form

$$\begin{aligned} &\int_{\Omega_j} (V_t + F'(U))\phi \mathrm{d}x + \int_{\Omega_j} W\phi_x \mathrm{d}x - \widehat{W}_{j+1}\phi_{j+1}^- + \widehat{W}_j\phi_j^+ = 0, \\ &\int_{\Omega_j} (U_t - V)\psi \mathrm{d}x = 0, \\ &\int_{\Omega_j} W\omega \mathrm{d}x + \int_{\Omega_j} U\omega_x \mathrm{d}x - \widehat{U}_{j+1}\omega_{j+1}^- + \widehat{U}_j\omega_j^+ = 0, \end{aligned} \tag{4.19}$$

where $\phi, \psi, \omega \in V_{\Delta x}^k(\Omega)$, $j = 0, 1, \cdots, N-1$. Since K_{13} and K_{31} are non-zero, the fluxes $\widehat{\boldsymbol{z}^{(1)}} = \widehat{U}$ and $\widehat{\boldsymbol{z}^{(3)}} = \widehat{W}$ (here $\widehat{\boldsymbol{z}^{(2)}}$ does not need to be defined) should be chosen as $\widehat{W} = W^+$, $\widehat{U} = U^-$, or $\widehat{W} = W^-$, $\widehat{U} = U^+$. By eliminating W from (4.19), we gain an ODEs with U and V as dependent variables. Combining a PRK scheme with coefficients (4.15) gives a PRK-DG scheme which can preserve the multi-symplectic structure of the system.

Example 4.2. Consider the "good" Boussinesq equation

$$u_{tt} = -u_{xxxx} + u_{xx} + (u^2)_{xx}, \ \ (t,x) \in \mathbb{R}^2, \tag{4.20}$$

which can be recast as [6]

$$M\boldsymbol{z}_t + K\boldsymbol{z}_x = \nabla_{\boldsymbol{z}} S(\boldsymbol{z}),$$

where

$$M = \begin{pmatrix} 0 & -1 & 0 & 0 \\ 1 & 0 & 0 & 0 \\ 0 & 0 & 0 & 0 \\ 0 & 0 & 0 & 0 \end{pmatrix}, \ K = \begin{pmatrix} 0 & 0 & -1 & 0 \\ 0 & 0 & 0 & -1 \\ 1 & 0 & 0 & 0 \\ 0 & 1 & 0 & 0 \end{pmatrix}, \ \boldsymbol{z} = \begin{pmatrix} u \\ v \\ p \\ q \end{pmatrix},$$

and $S(\boldsymbol{z}) = \frac{1}{2}(p^2 + q^2 - u^2 - \frac{2}{3}u^3)$.

Its DG variational discretization is

$$\begin{aligned} &-\int_{\Omega_j} (V_t + U^2 + U)\phi \mathrm{d}x + \int_{\Omega_j} P\phi_x \mathrm{d}x - \widehat{P}_{j+1}\phi_{j+1}^- + \widehat{P}_j\phi_j^+ = 0, \\ &\int_{\Omega_j} U_t\psi \mathrm{d}x + \int_{\Omega_j} Q\psi_x \mathrm{d}x - \widehat{Q}_{j+1}\psi_{j+1}^- + \widehat{Q}_j\psi_j^+ = 0, \\ &\int_{\Omega_j} P\eta \mathrm{d}x + \int_{\Omega_j} U\eta_x \mathrm{d}x - \widehat{U}_{j+1}\eta_{j+1}^- + \widehat{U}_j\eta_j^+ = 0, \\ &\int_{\Omega_j} Q\zeta \mathrm{d}x + \int_{\Omega_j} U\zeta_x \mathrm{d}x - \widehat{U}_{j+1}\zeta_{j+1}^- + \widehat{U}_j\zeta_j^+ = 0, \end{aligned} \tag{4.21}$$

where $\phi, \psi, \eta, \zeta \in V^k_{\Delta x}(\Omega),\ j = 0, 1, \cdots, N-1$. As the system is four-dimensional, the solution vector $\boldsymbol{z}$ can be partitioned in various ways. This leads to various choices of the fluxes. If we partition $\boldsymbol{z}$ as four parts, the fluxes can be taken as $\widehat{U} = U^+, \widehat{P} = P^-, \widehat{V} = V^+, \widehat{Q} = Q^-$, or $\widehat{U} = U^-, \widehat{P} = P^+, \widehat{V} = V^-, \widehat{Q} = Q^+$ for instance. If we partition $\boldsymbol{z}$ as two parts, i.e., $\boldsymbol{z} = (\boldsymbol{z^{(1)}}, \boldsymbol{z^{(2)}})$ with $\boldsymbol{z^{(1)}} = (u, v)$ and $\boldsymbol{z^{(2)}} = (p, q)$, then we can take the fluxes as $\widehat{U} = U^+,\ \widehat{V} = V^+,\ \widehat{P} = P^-,\ \widehat{Q} = Q^-$ or $\widehat{U} = U^-,\ \widehat{V} = V^-,\ \widehat{P} = P^+,\ \widehat{Q} = Q^+$. Eliminating P, Q gives an ODEs with U and V as dependent variables, then a PRK scheme with coefficients satisfying (4.15) can be used for the time discretization.

Example 4.3. Consider the Korteweg–de Vries (KdV) equation

$$u_t + \gamma u u_x + \epsilon^2 u_{xxx} = 0,\ \ (t, x) \in \mathbb{R}^2, \tag{4.22}$$

where γ, ϵ are two real numbers. By introducing $p_x = u$, $v = \epsilon u_x$, $w = \frac{1}{2} p_t + \epsilon v_x + \frac{1}{2}\gamma u^2$, we can rewrite the KdV equation as [32]

$$M\boldsymbol{z}_t + K\boldsymbol{z}_x = \nabla_{\boldsymbol{z}} S(\boldsymbol{z}),$$

where

$$M = \begin{pmatrix} 0 & \frac{1}{2} & 0 & 0 \\ -\frac{1}{2} & 0 & 0 & 0 \\ 0 & 0 & 0 & 0 \\ 0 & 0 & 0 & 0 \end{pmatrix},\ K = \begin{pmatrix} 0 & 0 & 0 & 1 \\ 0 & 0 & -\epsilon & 0 \\ 0 & \epsilon & 0 & 0 \\ -1 & 0 & 0 & 0 \end{pmatrix},\ \boldsymbol{z} = \begin{pmatrix} p \\ u \\ v \\ w \end{pmatrix}$$

and $S(\boldsymbol{z}) = \frac{1}{2} v^2 - uw + \frac{1}{6}\gamma u^3$.

By DG discretization in the temporal direction, we get the variational formulation

$$\begin{aligned}
&\int_{I_j} W_x \phi \mathrm{d}t = \frac{1}{2}\int_{I_j} U\phi_t \mathrm{d}t - \widehat{U}_{j+1}\phi^-_{j+1} + \widehat{U}_j \phi^+_j, \\
&-\epsilon \int_{I_j} V_x \psi \mathrm{d}t = \int_{I_j} (-w + \frac{1}{2}\gamma U^2)\psi \mathrm{d}t - \frac{1}{2}\int_{I_j} P\psi_t \mathrm{d}t + \widehat{P}_{j+1}\psi^-_{j+1} - \widehat{P}_j \psi^+_j, \\
&\int_{I_j} \epsilon U_x \eta \mathrm{d}t = \int_{I_j} V\eta \mathrm{d}t, \\
&\int_{I_j} P_x \eta \mathrm{d}t = \int_{I_j} U\eta \mathrm{d}t,
\end{aligned} \tag{4.23}$$

where $\phi, \psi, \eta, \zeta \in V^k_{\Delta t}(I),\ j = 0, 1, \cdots, N-1$. By considering the structure of the skew-symmetric matrix M, we naturally partition $\boldsymbol{z}$ into four parts and choose the numerical fluxes $\widehat{\boldsymbol{z}^{(1)}} = \widehat{P}$ and $\widehat{\boldsymbol{z}^{(2)}} = \widehat{U}$ (here both $\widehat{\boldsymbol{z}^{(3)}}$ and $\widehat{\boldsymbol{z}^{(4)}}$ do not need to be defined) from different directions, i.e., $\widehat{P} = P^-, \widehat{U} = U^+$ or $\widehat{P} = P^+, \widehat{U} = U^-$. We then get an ODEs (with suitable boundary conditions) with W, V, U, P as dependent variables, then a PRK scheme with coefficients satisfying (4.16) can be used for the spatial discretization.

5. DG methods for Schrödinger equation

In this section, taking the Schrödinger equation as a model problem, we investigate the numerical discretization by DG method and analyze its conservative properties.

Consider the following Schrödinger equation

$$\begin{cases} iu_t + u_{xx} + F'(|u|^2)u = 0, & (t, x) \in (0, \infty) \times [\mathcal{L}, \mathcal{R}], \\ u(0, x) = u_0(x), \end{cases} \tag{5.1}$$

where $F : \mathbb{R} \longrightarrow \mathbb{R}$ is a smooth function. Let $u = p + iq$, then we can get the multi-symplectic formulation of the Schrödinger equation [16]

$$M\boldsymbol{z}_t + K\boldsymbol{z}_x = \nabla_{\boldsymbol{z}} S(\boldsymbol{z}), \tag{5.2}$$

where $M = \begin{pmatrix} J & \mathbf{0} \\ \mathbf{0} & \mathbf{0} \end{pmatrix}$ with $J = \begin{pmatrix} 0 & 1 \\ -1 & 0 \end{pmatrix}$ and $K = \begin{pmatrix} \mathbf{0} & -I_2 \\ I_2 & \mathbf{0} \end{pmatrix}$, $\boldsymbol{z} = (p, q, v, w)^T$, $v = p_x$, $w = q_x$, and $S(\boldsymbol{z}) = \frac{1}{2}F(p^2 + q^2) + \frac{1}{2}(v^2 + w^2)$. It is known that the Schrödinger equation has an infinite number of conservation laws. With its multi-symplectic formulation (5.2), we list some of them:

(a) $\partial_t(\mathrm{d}p\wedge\mathrm{d}q)-\partial_x(\mathrm{d}p\wedge\mathrm{d}v+\mathrm{d}q\wedge\mathrm{d}w)=0$ (multi-symplectic conservation);
(b) $\partial_t[\frac{1}{2}(p^2+q^2)]+\partial_x(pw-qv)=0$ (charge conservation);
(c) $\partial_t[\frac{1}{2}F(p^2+q^2)-\frac{1}{2}(v^2+w^2)]+\partial_x(vp_t+wq_t)=0$ (energy conservation);
(d) $\partial_t(pw-qv)+\partial_x[F(p^2+q^2)+v^2+w^2-pq_t+qp_t]=0$ (momentum conservation).

By integrating these formulae with respect to x over the whole spatial domain, we can obtain the corresponding global conservation laws.

In what follows, we design the DG methods with the appropriate numerical fluxes so that the resulting discretization can preserve the discrete analogues of these conservation laws. The variational formulation of (5.2) is

$$\int_{\Omega_j}P_t\phi\mathrm{d}x=-\int_{\Omega_j}F'(P^2+Q^2)Q\,\phi\mathrm{d}x+\int_{\Omega_j}W\phi_x\mathrm{d}x-\widehat{W}_{j+1}\phi^-_{j+1}+\widehat{W}_j\phi^+_j, \tag{5.3}$$

$$\int_{\Omega_j}Q_t\psi\,\mathrm{d}x=\int_{\Omega_j}F'(P^2+Q^2)P\psi\,\mathrm{d}x-\int_{\Omega_j}V\psi_x\mathrm{d}x+\widehat{V}_{j+1}\psi^-_{j+1}-\widehat{V}_j\psi^+_j, \tag{5.4}$$

$$\int_{\Omega_j}V\tilde{\phi}\mathrm{d}x=-\int_{\Omega_j}P\tilde{\phi}_x\mathrm{d}x+\widehat{P}_{j+1}\tilde{\phi}^-_{j+1}-\widehat{P}_j\tilde{\phi}^+_j, \tag{5.5}$$

$$\int_{\Omega_j}W\tilde{\psi}\,\mathrm{d}x=-\int_{\Omega_j}Q\,\tilde{\psi}_x\mathrm{d}x+\widehat{Q}_{j+1}\tilde{\psi}^-_{j+1}-\widehat{Q}_j\tilde{\psi}^+_j, \tag{5.6}$$

where $\phi,\psi,\tilde{\phi},\tilde{\psi}\in V^k_{\Delta x}(\Omega)$ and $j=0,1,\cdots,N-1$.

We choose the following numerical fluxes

$$\widehat{P}=P^-,\ \widehat{Q}=Q^-;\ \widehat{V}=V^+,\ \widehat{W}=W^+, \tag{5.7}$$

or alternatively,

$$\widehat{P}=P^+,\ \widehat{Q}=Q^+;\ \widehat{V}=V^-,\ \widehat{W}=W^-. \tag{5.8}$$

Assume $\{x^j_\iota\}_{\iota=1}^{k+1}$ be $k+1$ distinct inner nodes in $\Omega_j=[x_j,x_{j+1}]$. We take the Lagrange interpolation polynomials

$$\varphi_i(x)=\prod_{\iota=1,\iota\neq i}^{k+1}\frac{x-x^j_\iota}{x^j_i-x^j_\iota},\quad x\in\Omega_j,\ i=1,2,\cdots,k+1 \tag{5.9}$$

as the local basis functions which then allow us to expand P, Q, V and W as

$$P=\sum_{i=1}^{k+1}P^j_i\varphi_i(x),\ Q=\sum_{i=1}^{k+1}Q^j_i\varphi_i(x),\ V=\sum_{i=1}^{k+1}V^j_i\varphi_i(x),\ W=\sum_{i=1}^{k+1}W^j_i\varphi_i(x),\ x\in\Omega_j. \tag{5.10}$$

Denote $\boldsymbol{P}^j=(P^j_1,\cdots,P^j_{k+1})^T$, $\boldsymbol{Q}^j=(Q^j_1,\cdots,Q^j_{k+1})^T$, $\boldsymbol{V}^j=(V^j_1,\cdots,V^j_{k+1})^T$, $\boldsymbol{W}^j=(W^j_1,\cdots,W^j_{k+1})^T$. We choose the interpolation nodes such that the first node x^j_1 coincides with x_j and the last one x^j_{k+1} coincides with x_{j+1}, which then provides $P^j_1=P^+_j$, $P^j_{k+1}=P^-_{j+1}$. In (5.5) we take $\tilde{\phi}=\varphi_i(x)$, $i=1,2,\cdots,k+1$, then it follows that

$$\boldsymbol{A}\boldsymbol{V}^j=-\boldsymbol{B}\boldsymbol{P}^j+\widehat{P}_{j+1}\boldsymbol{e}_{k+1}-\widehat{P}_j\boldsymbol{e}_1, \tag{5.11}$$

where $\boldsymbol{A}=(\int_{\Omega_j}\varphi_m(x)\varphi_n(x)\,\mathrm{d}x)$, $\boldsymbol{B}=(\int_{\Omega_j}\varphi'_m(x)\varphi_n(x)\,\mathrm{d}x)\in\mathbb{R}^{(k+1)\times(k+1)}$, $\boldsymbol{e}_\iota$ is the unit vector with ι-th element 1 and others 0. Here $\boldsymbol{A}$ is nonsingular (as it is a Gram matrix), thus from (5.11) we have

$$\boldsymbol{V}^j=-\boldsymbol{A}^{-1}\boldsymbol{B}\boldsymbol{P}^j+\widehat{P}_{j+1}\boldsymbol{A}^{-1}\boldsymbol{e}_{k+1}-\widehat{P}_j\boldsymbol{A}^{-1}\boldsymbol{e}_1. \tag{5.12}$$

Similarly, we have

$$\boldsymbol{W}^j=-\boldsymbol{A}^{-1}\boldsymbol{B}\boldsymbol{Q}^j+\widehat{Q}_{j+1}\boldsymbol{A}^{-1}\boldsymbol{e}_{k+1}-\widehat{Q}_j\boldsymbol{A}^{-1}\boldsymbol{e}_1. \tag{5.13}$$

By virtue of (5.12)–(5.13), from Eqs. (5.3)–(5.6) we obtain a system of ODEs with P, Q as dependent variables.

Next, let us show the conservative properties of the DG method introduced above.

Theorem 5.1 *(Charge conservation). Under the periodic or null boundary conditions, i.e.,* $u(t, x+\mathcal{L}) = u(t, x+\mathcal{R})$ *or* $u(t, \mathcal{L}) = u(t, \mathcal{R}) \equiv 0$*, the DG semi-discretized scheme (5.3)–(5.6) with the numerical fluxes (5.7) (or (5.8)) preserves the following discrete global charge conservation law*

$$\mathbb{C}(t) = \mathbb{C}(t_0), \tag{5.14}$$

where $\mathbb{C}(t) = \int_\Omega \frac{1}{2}|U(t,x)|^2 \mathrm{d}x$ *and* $U = P(t,x) + iQ(t,x)$.

Proof. Here, we only show the proof for the DG scheme with the numerical fluxes (5.7). In (5.3)–(5.6), taking $\phi = P$, $\psi = Q$, $\tilde{\phi} = W$, $\tilde{\psi} = V$ gives rise to

$$\int_{\Omega_j} P_t P \mathrm{d}x = -\int_{\Omega_j} F'(|U|^2) Q\, P \mathrm{d}x + \int_{\Omega_j} W P_x \mathrm{d}x - W_{j+1}^+ P_{j+1}^- + W_j^+ P_j^+, \tag{5.15}$$

$$\int_{\Omega_j} Q_t Q \,\mathrm{d}x = \int_{\Omega_j} F'(|U|^2) P\, Q \,\mathrm{d}x - \int_{\Omega_j} V Q_x \mathrm{d}x + V_{j+1}^+ Q_{j+1}^- - V_j^+ Q_j^+, \tag{5.16}$$

$$\int_{\Omega_j} V W \mathrm{d}x = -\int_{\Omega_j} P W_x \mathrm{d}x + P_{j+1}^- W_{j+1}^- - P_j^- W_j^+, \tag{5.17}$$

$$\int_{\Omega_j} W V \mathrm{d}x = -\int_{\Omega_j} Q V_x \mathrm{d}x + Q_{j+1}^- V_{j+1}^- - Q_j^- V_j^+. \tag{5.18}$$

Using the integration by parts, it follows from (5.17) and (5.18) that

$$\begin{aligned} \int_{\Omega_j} V W \mathrm{d}x &= \int_{\Omega_j} P_x W \mathrm{d}x + P_j^+ W_j^+ - P_j^- W_j^+, \\ \int_{\Omega_j} W V \mathrm{d}x &= \int_{\Omega_j} Q_x V \mathrm{d}x + Q_j^+ V_j^+ - Q_j^- V_j^+. \end{aligned} \tag{5.19}$$

By combining (5.15), (5.16) with (5.19) and summing up the formulae for all Ω_j, we derive

$$\frac{d}{dt}\int_\Omega \frac{1}{2}|U(t,x)|^2 \mathrm{d}x = P_0^- W_0^+ - P_N^- W_N^+ + Q_N^- V_N^+ - Q_0^- V_0^+$$

which vanishes under the periodic or null boundary conditions. We can derive a similar result when the numerical fluxes (5.8) are used. This completes the proof of this theorem. □

The above theorem can directly address the following conclusion.

Corollary 5.1 *(L^2 stability). Under the periodic or null boundary conditions, the semi-discretized scheme (5.3)–(5.6) with numerical fluxes (5.7) (or (5.8)) satisfies the L^2 stability, that is*

$$\frac{d}{dt}\int_\Omega |U(t,x)|^2 \mathrm{d}x = 0.$$

Remark 5.1. In order to preserve the global charge $\mathbb{C}(t)$, there exist other choices of the numerical fluxes besides (5.7) and (5.8). For example, we can choose the fluxes as follows

$$\widehat{P} = P^+,\ \widehat{Q} = Q^-,\ \widehat{V} = V^+,\ \widehat{W} = W^-, \tag{5.20}$$

$$\widehat{P} = P^-,\ \widehat{Q} = Q^+,\ \widehat{V} = V^-,\ \widehat{W} = W^+, \tag{5.21}$$

$$\widehat{P} = P^\lambda,\ \widehat{Q} = Q^{1-\lambda},\ \widehat{V} = V^\lambda,\ \widehat{W} = W^{1-\lambda}, \tag{5.22}$$

where $\varphi^\lambda = \lambda\varphi^+ + (1-\lambda)\varphi^-$ with $\lambda \in (0,1)$. These DG methods with fluxes (5.20)–(5.22) possess L^2 stability, but they do not preserve the energy conservation except the case of (5.22) with $\lambda = \frac{1}{2}$.

Theorem 5.2 *(Energy conservation). Under the periodic or null boundary conditions, the DG semi-discrete scheme (5.3)–(5.6) with the numerical fluxes (5.7) (or (5.8)) preserves the following discrete global energy conservation law*

$$\mathbb{E}(t) = \mathbb{E}(t_0), \tag{5.23}$$

where $\mathbb{E}(t) = \int_\Omega [\frac{1}{2}F(P^2(t,x) + Q^2(t,x)) - \frac{1}{2}(V^2(t,x) + W^2(t,x))]\mathrm{d}x$.

Proof. The proof is similar to Theorem 5.1. The result can be derived by letting $\phi = Q_t, \psi = P_t$ in (5.3)–(5.4) and taking $\tilde{\phi} = V, \tilde{\psi} = W$ after differentiating (5.5)–(5.6) with respect to t. □

Remark 5.2. To get the exact conservation of the global energy $\mathbb{E}(t)$, besides (5.7) and (5.8) the other choices of numerical fluxes can be

$$\widehat{P} = P^+,\ \widehat{Q} = Q^-,\ \widehat{V} = V^-,\ \widehat{W} = W^+, \tag{5.24}$$

$$\widehat{P} = P^-,\ \widehat{Q} = Q^+,\ \widehat{V} = V^+,\ \widehat{W} = W^-, \tag{5.25}$$

$$\widehat{P} = P^\lambda,\ \widehat{Q} = Q^{1-\lambda},\ \widehat{V} = V^{1-\lambda},\ \widehat{W} = W^\lambda, \tag{5.26}$$

where $\varphi^\lambda = \lambda\varphi^+ + (1-\lambda)\varphi^-$ with $\lambda \in (0,1)$. However, except the case of (5.26) with $\lambda = \frac{1}{2}$ we do not have the exact charge conservation.

By the discussions in the previous section we directly obtain the following results.

Theorem 5.3. *For the Schrödinger equation (5.1), we discretize it by the DG method (5.3)–(5.6) with fluxes (5.7) (or (5.8)) in space and a symplectic RK method in time, then the resulting full-discrete scheme is multi-symplectic. Moreover, if F is a linear function, then the charge* $\mathbb{C}(t)$ *and energy* $\mathbb{E}(t)$ *can be preserved exactly by the full discretization.*

Proof. The first statement can be seen from Theorem 4.1 and Remark 4.2. As the charge and energy are quadratic, symplectic RK methods can preserve these invariants exactly (see Theorem 2.2 and 4.3 in [10]). □

Remark 5.3. We can also partition $\boldsymbol{z}$ into four parts to get a multi-symplectic scheme from the DG method. In this case, we can take the following fluxes

$$\widehat{P} = P^+,\ \widehat{V} = V^-;\ \widehat{Q} = Q^-,\ \widehat{W} = W^+,$$

or

$$\widehat{P} = P^-,\ \widehat{V} = V^+;\ \widehat{Q} = Q^+,\ \widehat{W} = W^-.$$

For these two cases, the energy $\mathbb{E}(t)$ is exactly preserved by the DG semi-discrete scheme (see Remark 5.2).

6. Numerical experiments

In this section, we present the numerical experiments by applying the DG methods to Hamiltonian ODEs and PDEs. We start this section by showing the numerical results for the ODEs case.

Example 6.1. Consider the Hénon–Heiles model which was presented in [10] to describe the stellar motion. The model can be written as a Hamiltonian ODEs

$$\boldsymbol{z}_t = J^{-1}\nabla_{\boldsymbol{z}} H(\boldsymbol{z})$$

with $\boldsymbol{z} = (p_1, p_2, q_1, q_2)^T \in \mathbb{R}^4$, $H(\boldsymbol{z}) = \frac{1}{2}(p_1^2 + p_2^2) + \frac{1}{2}(q_1^2 + q_2^2) + q_1^2 q_2 - \frac{1}{3}q_2^3$. We take $\boldsymbol{z}(0) = (0, 0, 0.1, -0.5)$ as the initial value.

We use the following four choices of fluxes: $(P_1^-, P_2^-, Q_1^+, Q_2^+)$, $(P_1^-, P_2^+, Q_1^+, Q_2^-)$, $(P_1^+, P_2^-, Q_1^-, Q_2^+)$, $(P_1^+, P_2^+, Q_1^-, Q_2^-)$ to derive the symplectic DG method. The numerical results computed by the 2-degree DG schemes are illustrated in Fig. 6.1 which exhibits the bounded small energy errors over long-time interval. It is observed that with the fluxes (3.3) and (3.4) the numerical solutions provide the optimal energy conservation.

We also compare the numerical results of the 2-degree DG method with flux (3.3) and the explicit Nyström Runge–Kutta scheme of order 5 in Fig. 6.2. It is observed that our DG method which is symplectic and of order 5 can preserve the energy up to 10^{-10} over the long time, while the energy computed by the Nyström Runge–Kutta scheme produces a linear drift along with the time.

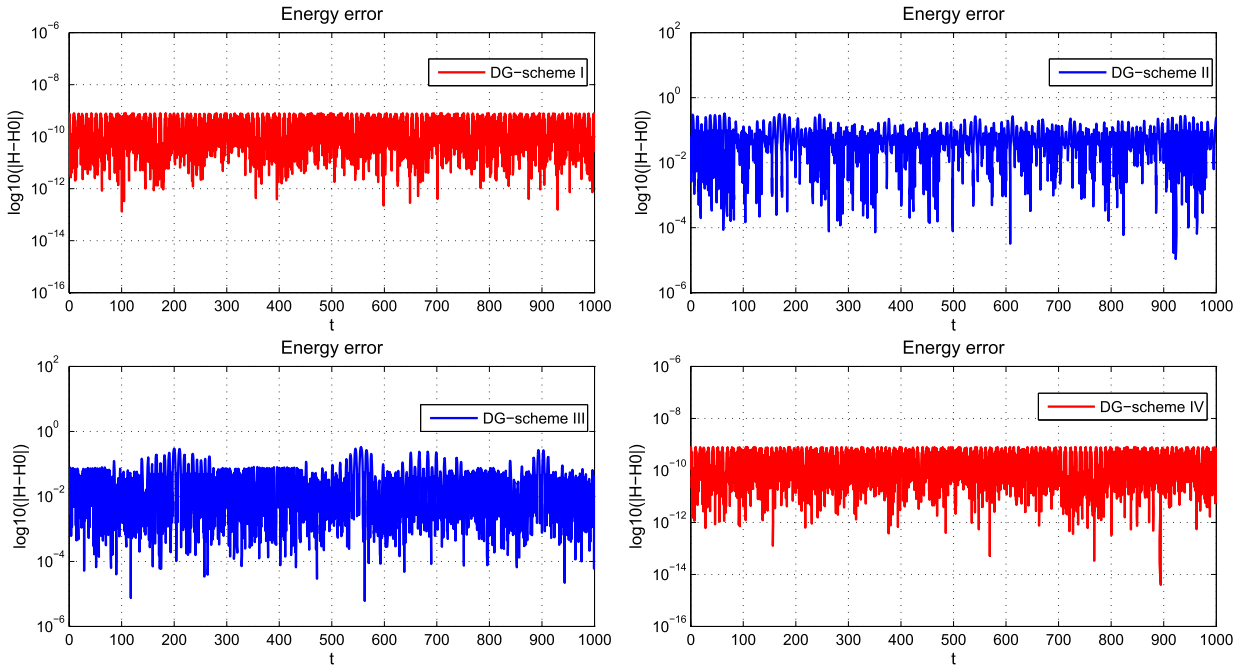

Fig. 6.1. Energy errors by DG schemes with various numerical fluxes: DG-scheme I with $(P_1^-, P_2^-, Q_1^+, Q_2^+)$ (see also (3.3)); DG-scheme II with $(P_1^-, P_2^+, Q_1^+, Q_2^-)$; DG-scheme III with $(P_1^+, P_2^-, Q_1^-, Q_2^+)$; DG-scheme IV with $(P_1^+, P_2^+, Q_1^-, Q_2^-)$ (see also (3.4)). The step size is $h = 0.1$.

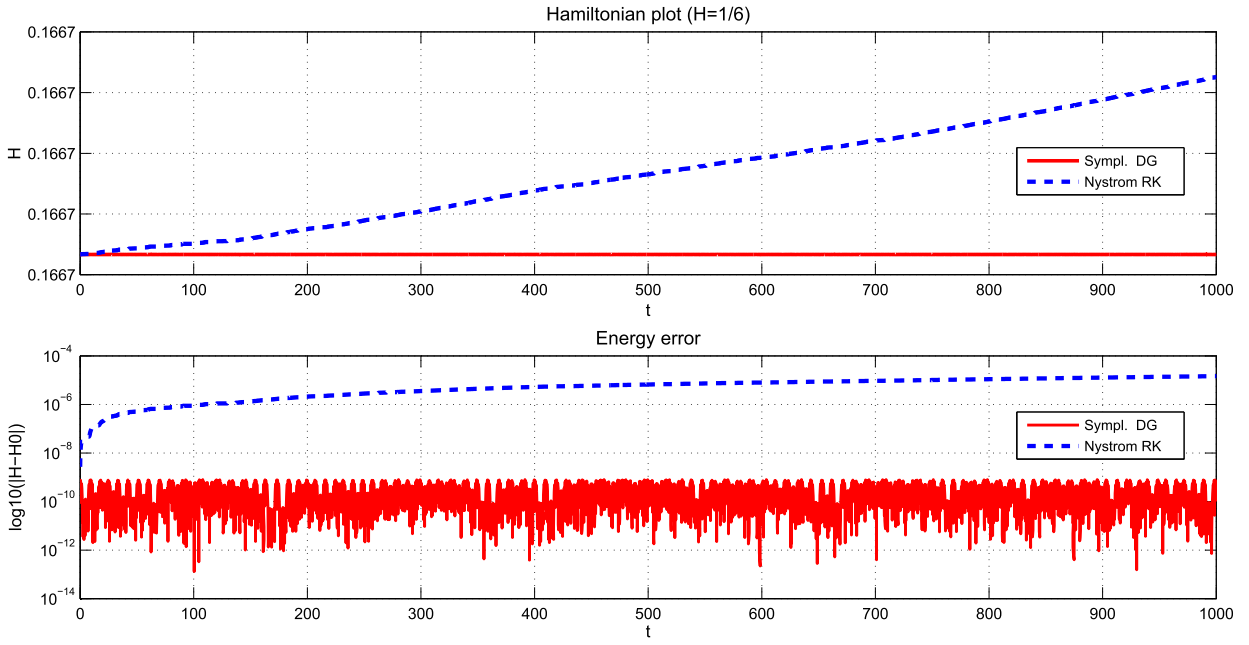

Fig. 6.2. Energy and errorcomparison between the DG method with fluxes $(P_1^-, P_2^-, Q_1^+, Q_2^+)$ (see also (3.3)) and the Nyström Runge–Kutta scheme with step size $h = 0.1$.

Example 6.2. Consider the linear Schrödinger equation

$$iu_t + u_{xx} + u = 0, \quad (t, x) \in (0, \infty) \times [-\frac{\pi}{2}, \frac{\pi}{2}], \tag{6.1}$$

with $u(0, x) = \sin(2x)$ and the periodic boundary conditions.

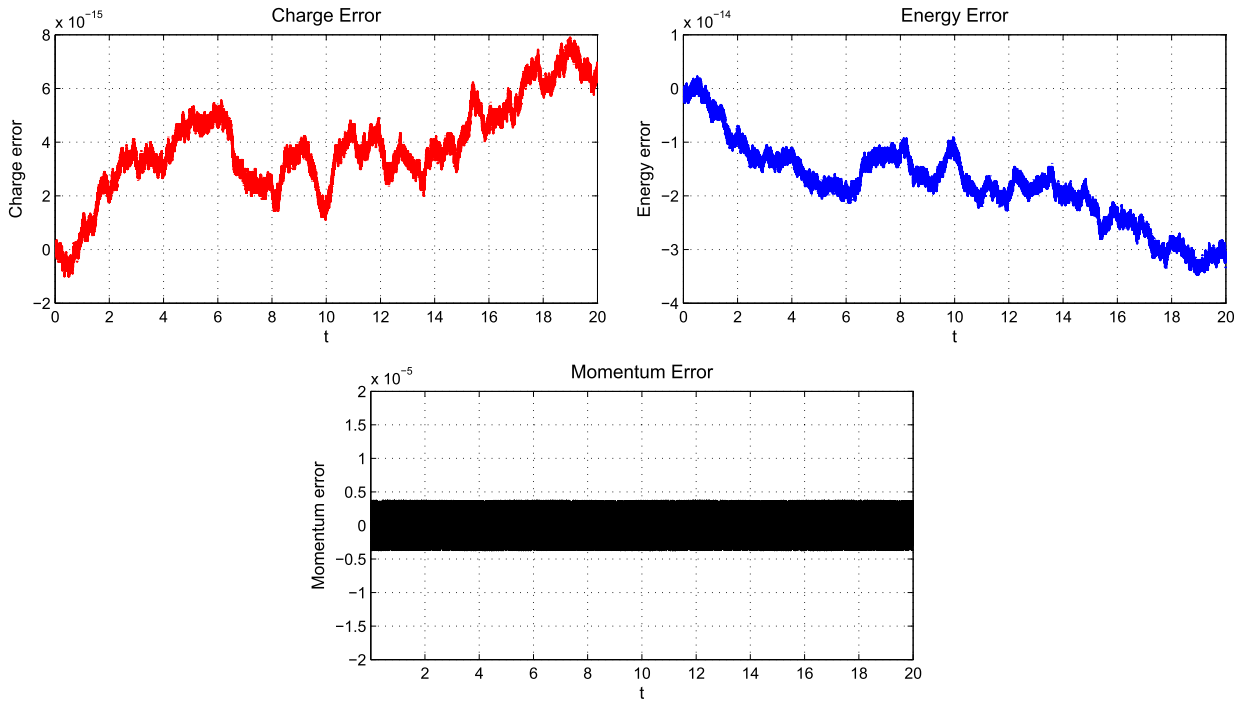

Fig. 6.3. Errors of three invariants for linear Schrödinger equation by the 2-degree DG method with fluxes (P^-, Q^-, V^+, W^+) (see also (5.7)) combining the implicit midpoint rule for time integration.

We take the 2-degree DG method with $\Delta x = 0.05\pi$ for the spatial discretization and the implicit midpoint rule (a well-known 2-order symplectic RK method) with $\Delta t = 0.0001$ for the time integration. We use the DG methods with four different fluxes: (5.7), (5.20), (5.22) ($\lambda = 1/2$) and (5.24). For this linear problem, the global charge $\mathbb{C}(t)$, energy $\mathbb{E}(t)$ and momentum $\mathbb{M}(t)$ (which is $\int_\Omega (PW - QV)dx$) are quadratic. If we choose the DG method with fluxes (5.7), then the resulting numerical scheme is multi-symplectic and can preserve both the charge and energy exactly (see Theorem 5.3). This is verified by Fig. 6.3. If we apply the DG method with flux (5.20), then we only get the charge conservation, see Fig. 6.4. For this case, it is surprising to see in Fig. 6.5 that the DG discretization with the use of (5.22) ($\lambda = 1/2$) can preserve three invariants. However, the momentum conservation has not been proven theoretically. It can be noticed clearly from the next nonlinear example. With the fluxes (5.24), the energy conservation is shown in Fig. 6.6 which is confirmed with Remark 5.2.

Example 6.3. Consider the following cubic nonlinear Schrödinger equation

$$iu_t + u_{xx} + 2|u|^2 u = 0, \ (t, x) \in (0, \infty) \times [-25, 25] \tag{6.2}$$

with the k-soliton initial value condition

$$u(0, x) = \sum_{\iota=1}^{k} \operatorname{sech}(x - x_\iota) \exp\left(2ic_\iota(x - x_\iota)\right), x \in [-25, 25], \tag{6.3}$$

We consider the single and double soliton cases, i.e. $k = 1$ and $k = 2$ in (6.3). We take $x_1 = -10$, $c_1 = 1$, $x_2 = 10$ and $c_2 = -1$. We still use the periodic boundary conditions and exploit the implicit midpoint rule for the time integration. The spatial and temporal step size are taken as $\Delta x = 0.4$ and $\Delta t = 0.001$, respectively.

In Figs. 6.7 and 6.8, we show the errors of three invariants computed by the 2-degree DG method with fluxes (5.7). From the numerical results, it is observed that the charge conservation can be preserved up to round error for both the single and double soliton cases. Though the other two invariants can not be preserved exactly, their errors can be bounded over long time. We show that the numerical discretization derived by the DG scheme with fluxes (5.20) is charge-preserving which has been well confirmed in Figs. 6.9 and 6.10.

In Figs. 6.11 and 6.12, we provide the numerical results by using DG method with fluxes (5.22) ($\lambda = 1/2$). It is observed that the method can preserve the momentum conservation exactly for the double soliton problem of the nonlinear system. However, this method fails to preserve the momentum of the nonlinear problem for the single soliton case. Comparing with other DG methods, the DG method with fluxes (5.22) ($\lambda = 1/2$) behaves well in the conservation of three invariants. This can be explained by some symmetry inherited by this method. However, Fig. 6.18 exhibits that the shape of the double

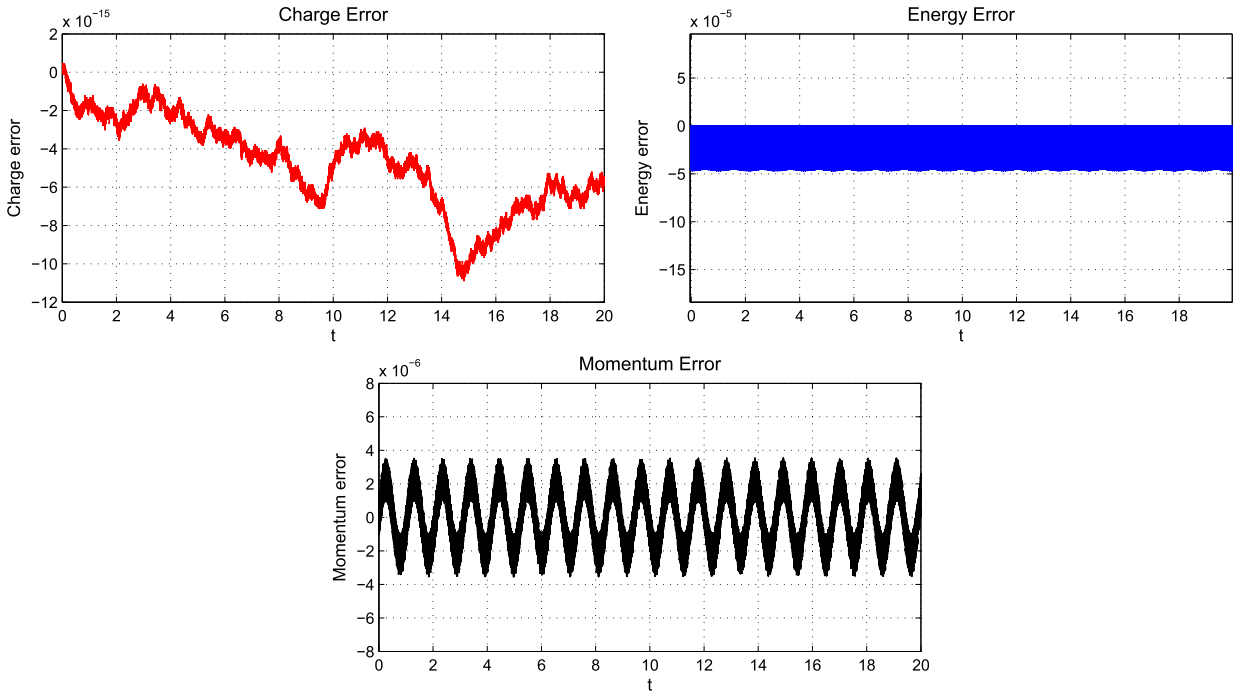

Fig. 6.4. Errors of three invariants for linear Schrödinger equation by the 2-degree DG method with fluxes (P^+, Q^-, V^+, W^-) (see also (5.20)) combining the implicit midpoint rule for time integration.

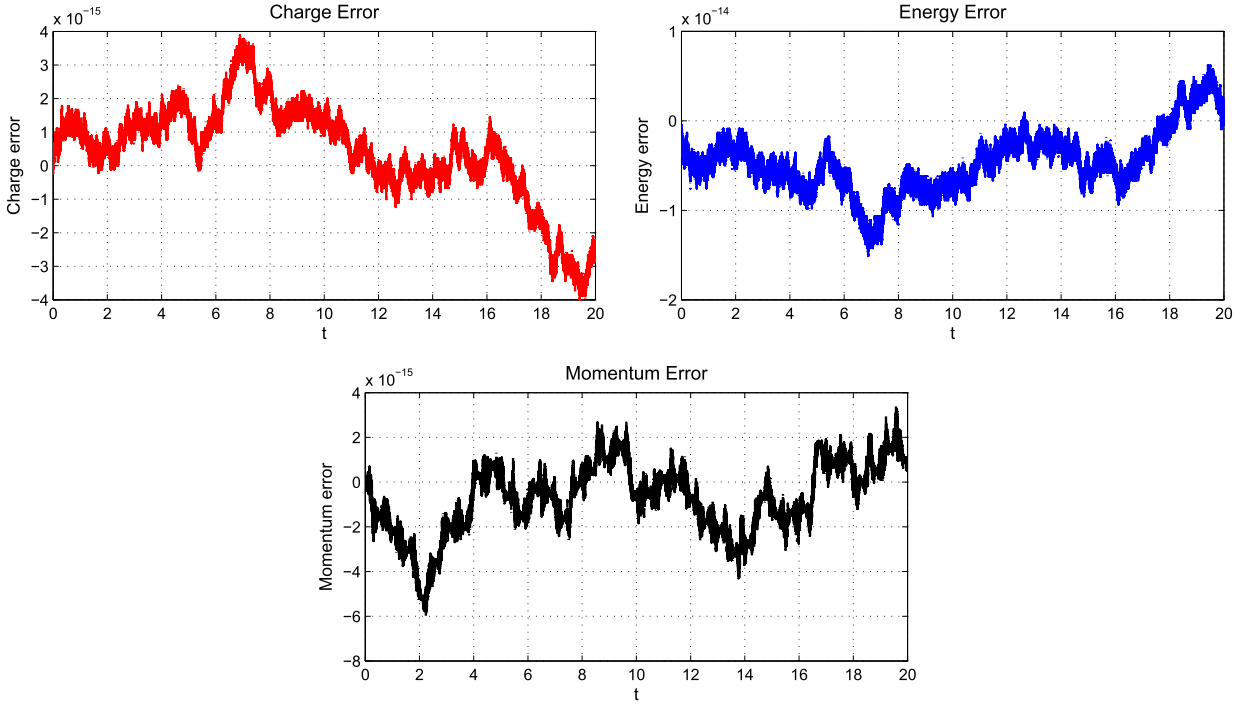

Fig. 6.5. Errors of three invariants for linear Schrödinger equation by the 2-degree DG method with fluxes $(P^{1/2}, Q^{1/2}, V^{1/2}, W^{1/2})$ (see also (5.22)) combining the implicit midpoint rule for time integration.

soliton looks somewhat not smooth after collision when a coarse spatial grid is used. Thus, the smaller step size should be used for producing the accurate shapes of the double soliton.

Figs. 6.13 and 6.14 are devoted to showing the numerical results of DG scheme with fluxes (5.24) which results in a multi-symplectic scheme after the implicit midpoint rule being exploited for the time discretization. Differently from

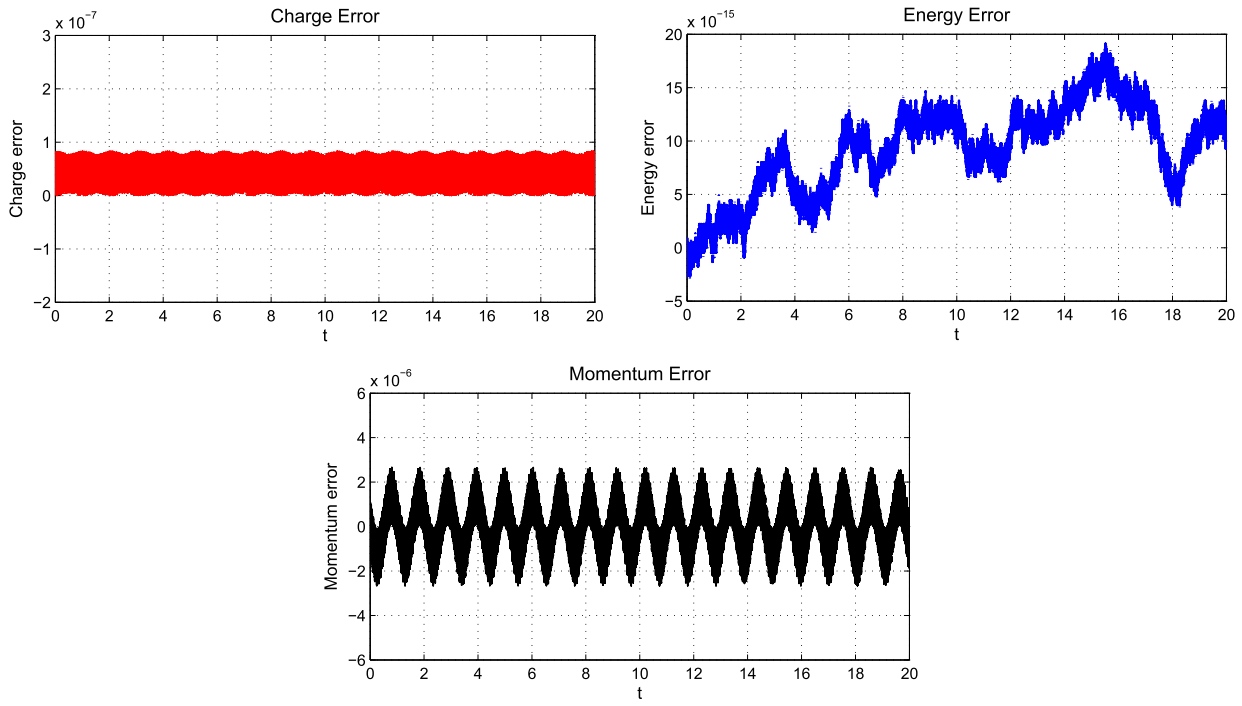

Fig. 6.6. Errors of three invariants for linear Schrödinger equation by the 2-degree DG method with fluxes (P^+, Q^-, V^-, W^+) (see also (5.24)) combining the implicit midpoint rule for time integration.

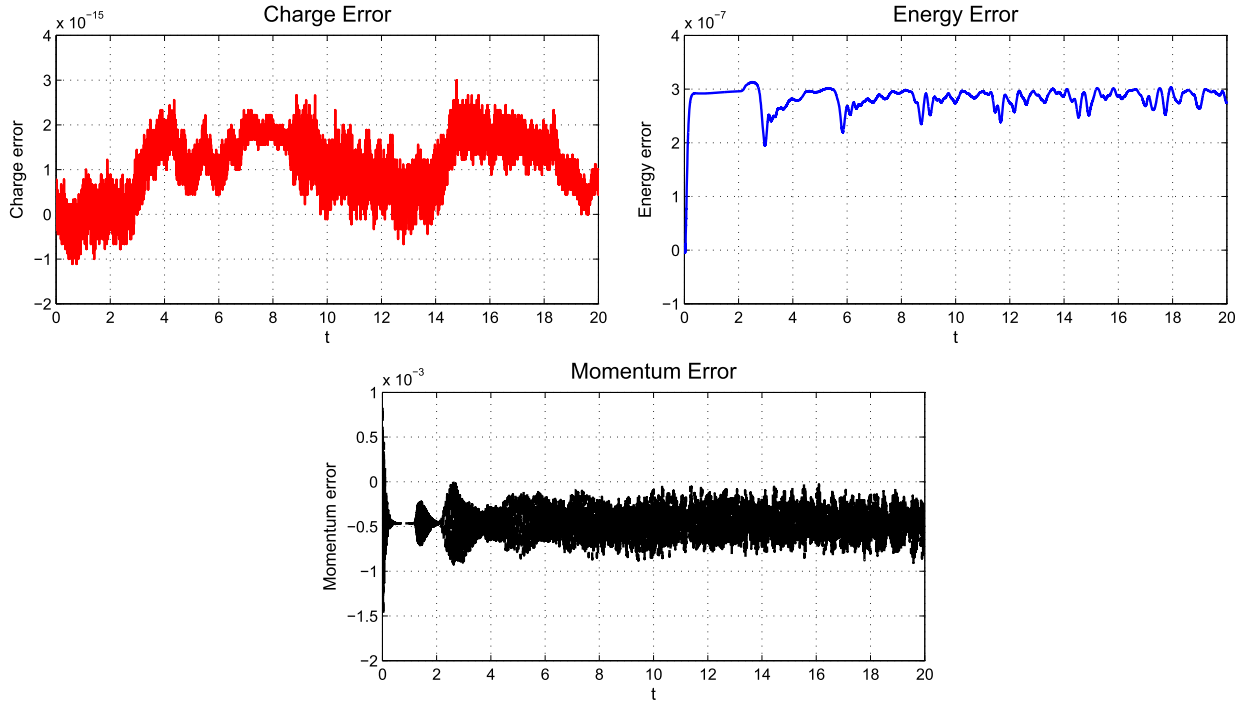

Fig. 6.7. Errors of three invariants of the single soliton of nonlinear Schrödinger equation by the 2-degree DG method with fluxes (P^-, Q^-, V^+, W^+) (see also (5.7)) combining the implicit midpoint rule for time integration, with the step sizes $\Delta x = 0.4$, $\Delta t = 0.001$.

the linear problem, the energy in the nonlinear case is not quadratic. Though we don't expect the numerical method to preserve the exact energy conservation, it is observed that the error of energy is smaller than other two invariants even for the double soliton case. We compare our methods with a well-known RK-DG method presented in [33], which is obtained

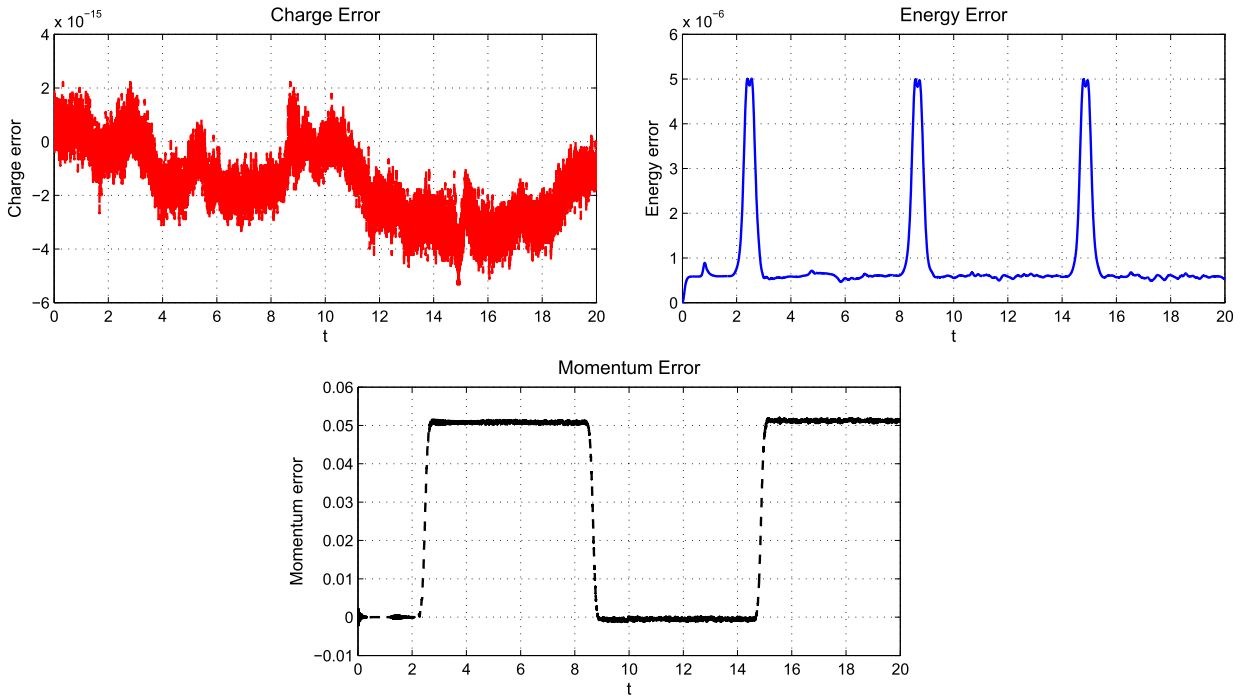

Fig. 6.8. Errors of three invariants of the double soliton of nonlinear Schrödinger equation by the 2-degree DG method with fluxes (P^-, Q^-, V^+, W^+) (see also (5.7)) combining the implicit midpoint rule for time integration, with the step sizes $\Delta x = 0.4$, $\Delta t = 0.001$.

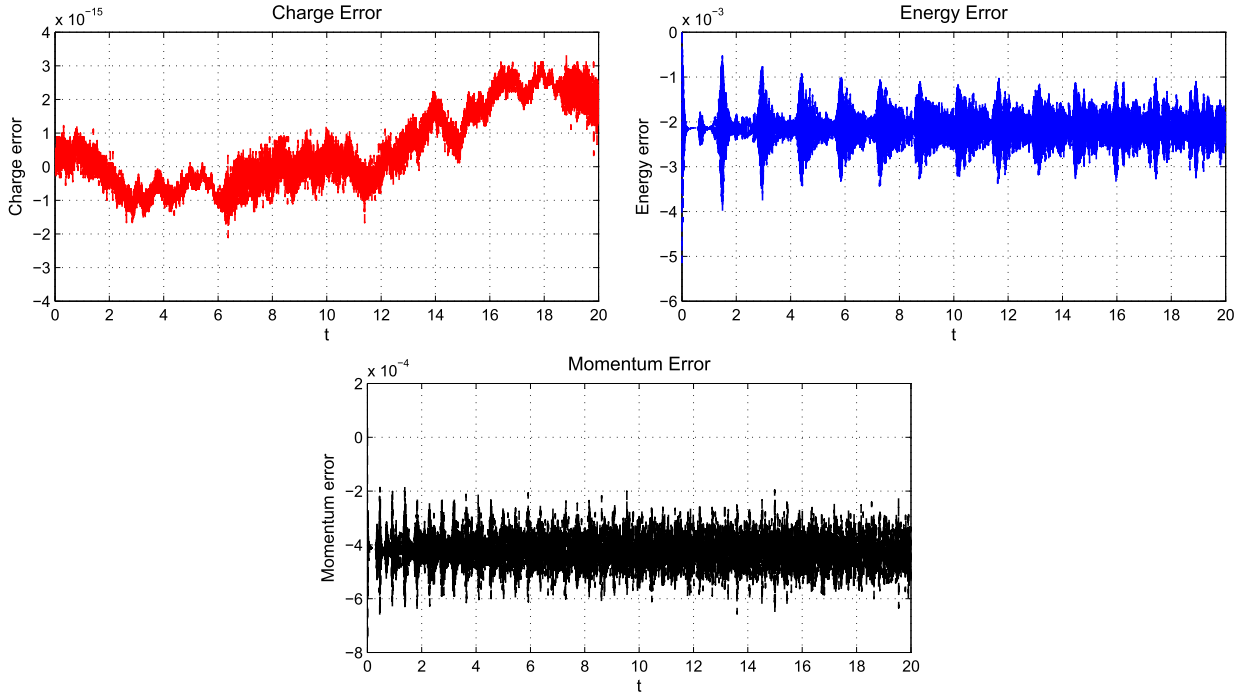

Fig. 6.9. Errors of three invariants of the single soliton of nonlinear Schrödinger equation by the 2-degree DG method with fluxes (P^+, Q^-, V^+, W^-) (see also (5.20)) combining the implicit midpoint rule for time integration, with the step sizes $\Delta x = 0.4$, $\Delta t = 0.001$.

by using the same spatial DG discretization but applying a 3-order RK scheme with strong nonlinear stability in time [24]. We can see from Figs. 6.15 and 6.16 that our method has a better conservation of the invariants.

We use Fig. 6.17 to illustrate the evolution of the single and double solitons, the left one gives the propagation of the single soliton, while the right one provides the collision process of a double soliton. It is observed that for both cases the

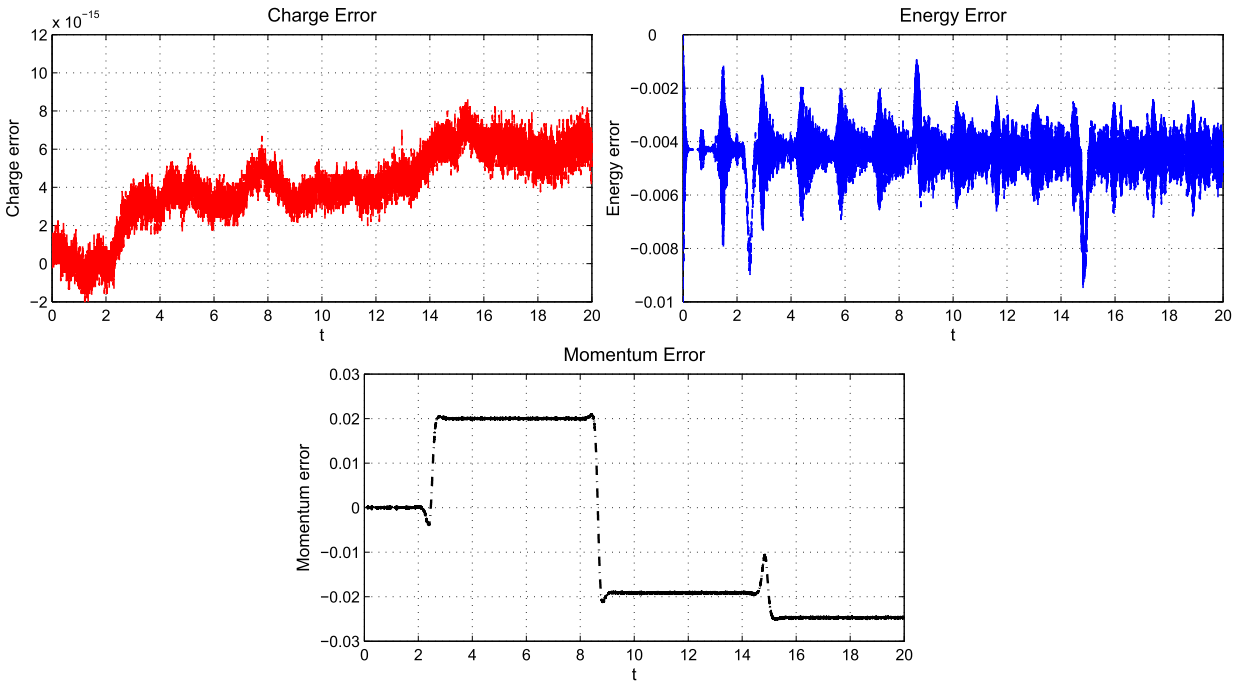

Fig. 6.10. Errors of three invariants of the double soliton of nonlinear Schrödinger equation by the 2-degree DG method with fluxes (P^+, Q^-, V^+, W^-) (see also (5.20)) combining the implicit midpoint rule for time integration, with the step sizes $\Delta x = 0.4$, $\Delta t = 0.001$.

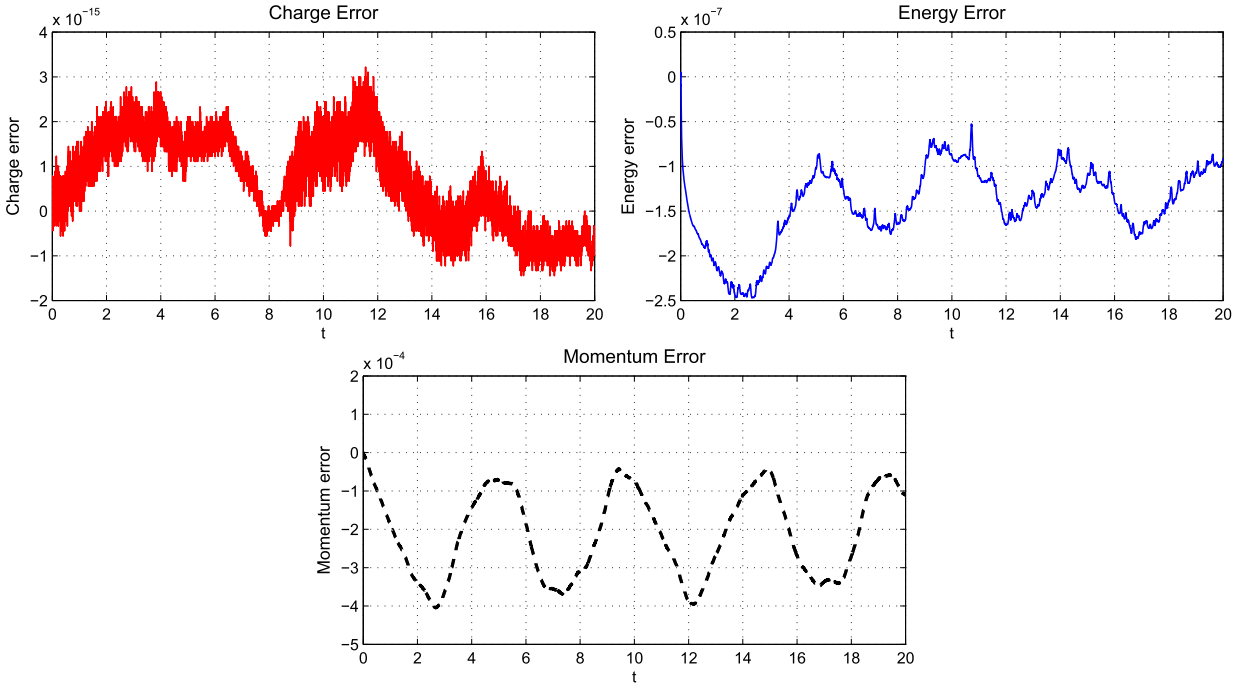

Fig. 6.11. Errors of three invariants of the single soliton of nonlinear Schrödinger equation by the 2-degree DG method with fluxes $(P^{1/2}, Q^{1/2}, V^{1/2}, W^{1/2})$ (see also (5.22)) combining the implicit midpoint rule for time integration, with the step sizes $\Delta x = 0.4$, $\Delta t = 0.001$.

numerical solutions can be reproduced perfectly. Here we only provide the results of the DG method with fluxes (5.7), as the results of other methods (excluding the case with (5.22) ($\lambda = 1/2$)) are similar. These figures illustrate that those algorithms which can preserve the conservative properties of the original system can capture the solution character very well.

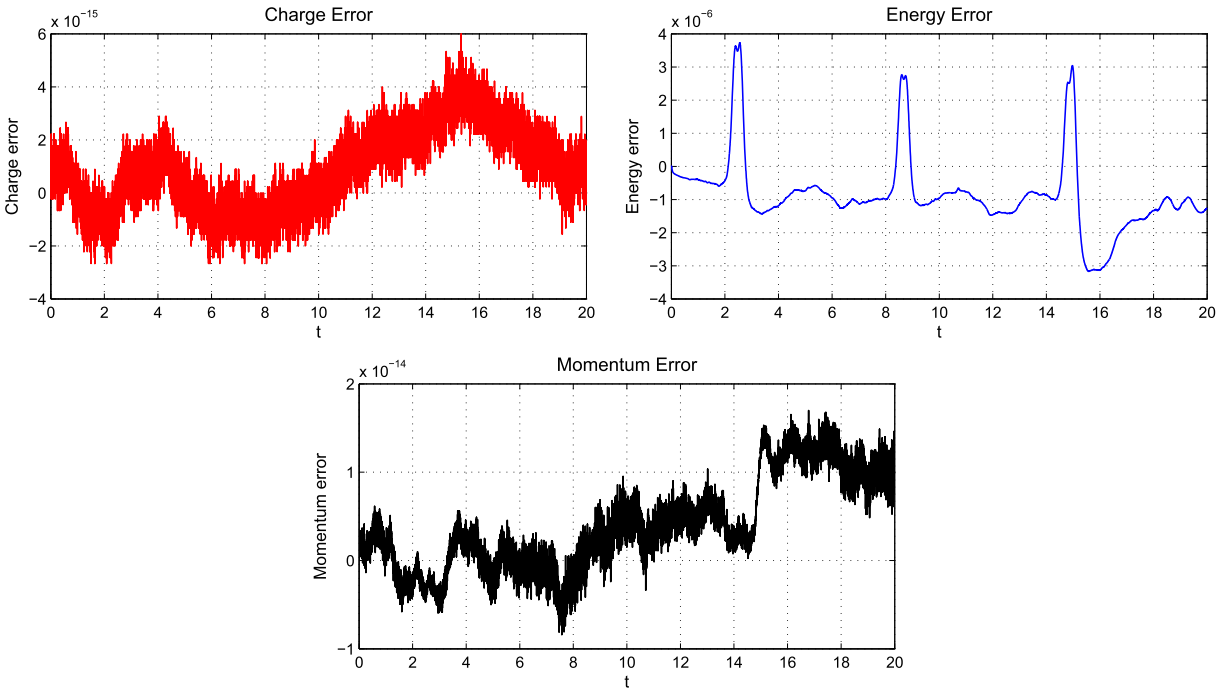

Fig. 6.12. Errors of three invariants of the double soliton of nonlinear Schrödinger equation by the 2-degree DG method with fluxes $(P^{1/2}, Q^{1/2}, V^{1/2}, W^{1/2})$ (see also (5.22)) combining the implicit midpoint rule for time integration, with the step sizes $\Delta x = 0.4$, $\Delta t = 0.001$.

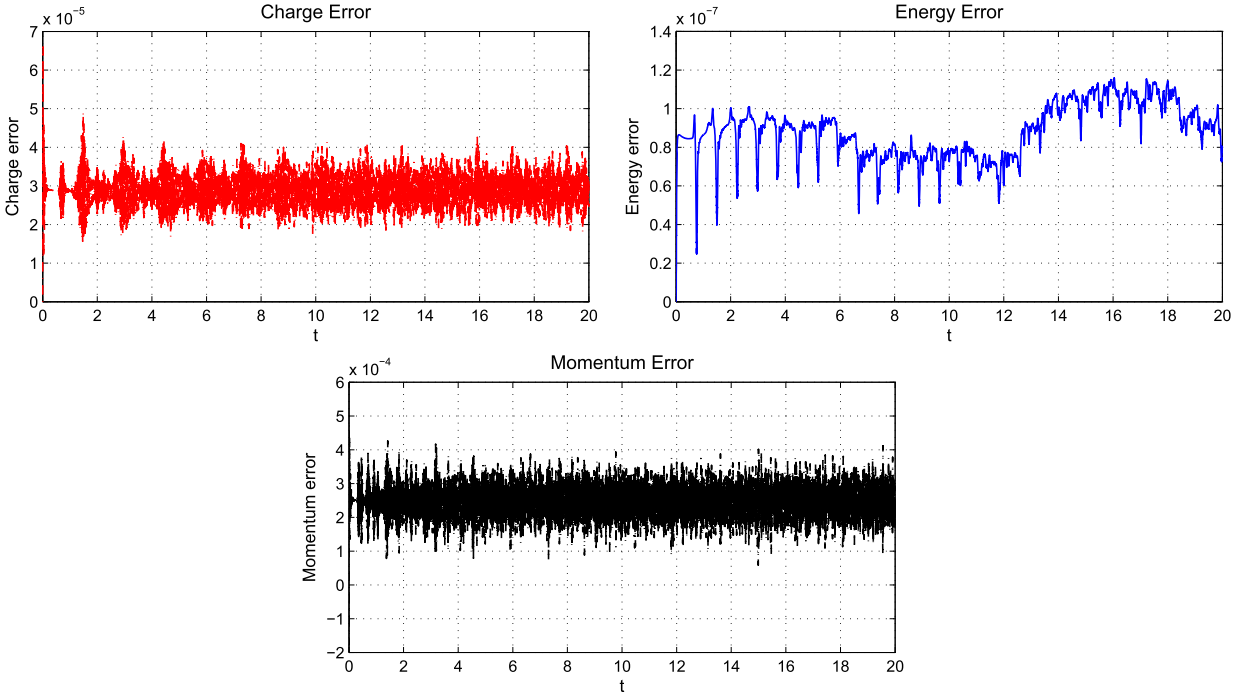

Fig. 6.13. Errors of three invariants of the single soliton of nonlinear Schrödinger equation by the 2-degree DG method with fluxes (P^+, Q^-, V^-, W^+) (see also (5.24)) combining the implicit midpoint rule for time integration, with the step sizes $\Delta x = 0.4$, $\Delta t = 0.001$.

7. Concluding remarks

We have developed the discontinuous Galerkin (DG) methods for solving Hamiltonian ODEs and PDEs in the current paper. It is shown that the DG approach can provide a new framework in which we can construct, analyze and understand the

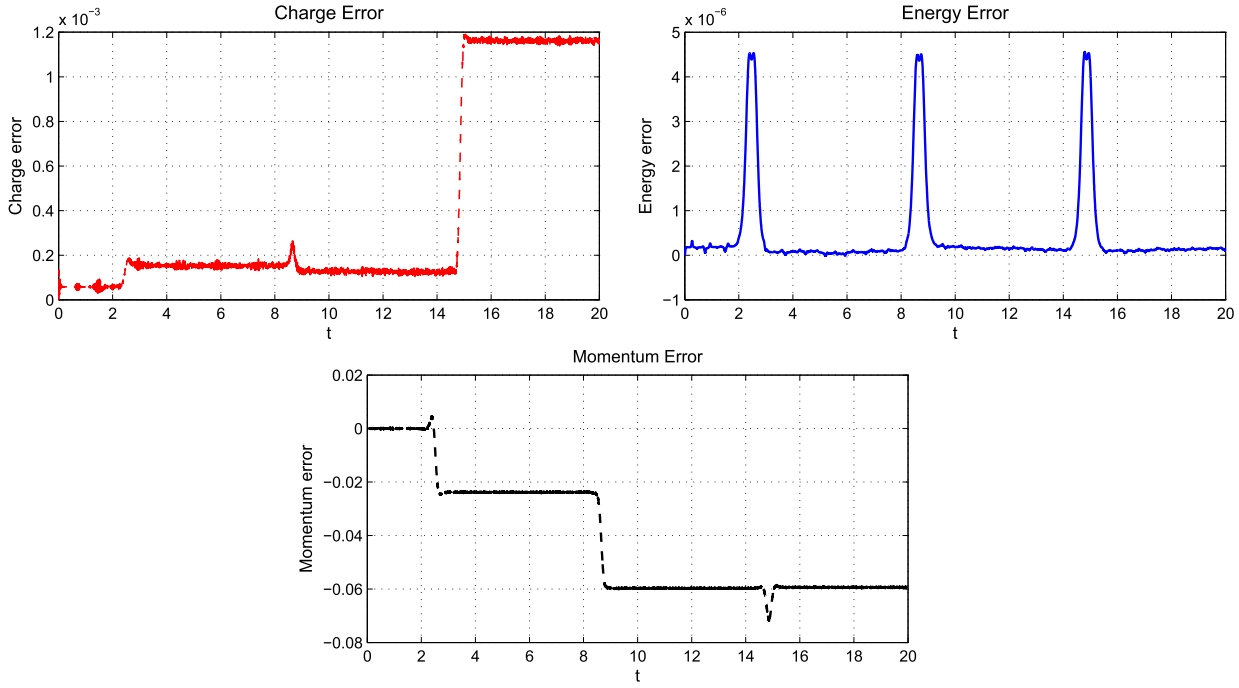

Fig. 6.14. Errors of three invariants of the double soliton of nonlinear Schrödinger equation by the 2-degree DG method with fluxes (P^+, Q^-, V^-, W^+) (see also (5.24)) combining the implicit midpoint rule for time integration, with the step sizes $\Delta x = 0.4$, $\Delta t = 0.001$.

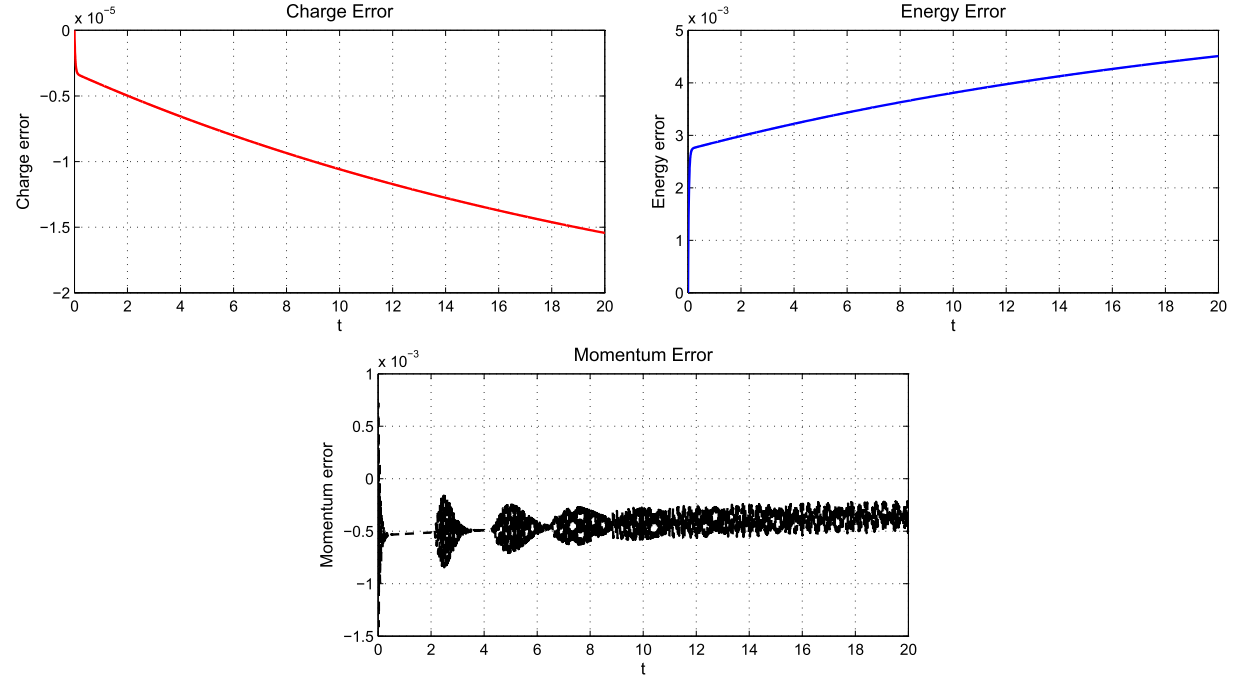

Fig. 6.15. Errors of three invariants of the single soliton of nonlinear Schrödinger equation by the 2-degree DG method with fluxes (P^-, Q^-, V^+, W^+) (see also (5.7)) combining the 3-order strong stability preserving Runge–Kutta method for time integration, with the step sizes $\Delta x = 0.4$, $\Delta t = 0.001$.

symplectic and multi-symplectic numerical methods. It is shown that the DG approach can be applied to Hamiltonian ODEs to design the symplectic methods, and the resulting algorithms are equivalent to high-order partitioned Runge–Kutta (PRK) schemes. Moreover, it is interesting to see that different symplectic schemes can be obtained by using different quadrature formulae. This study by DG discretization has been generalized to Hamiltonian PDEs. The resulting numerical schemes are shown to be equivalent to time-space multi-symplectic PRK schemes, which can be seen as the natural generalization of the

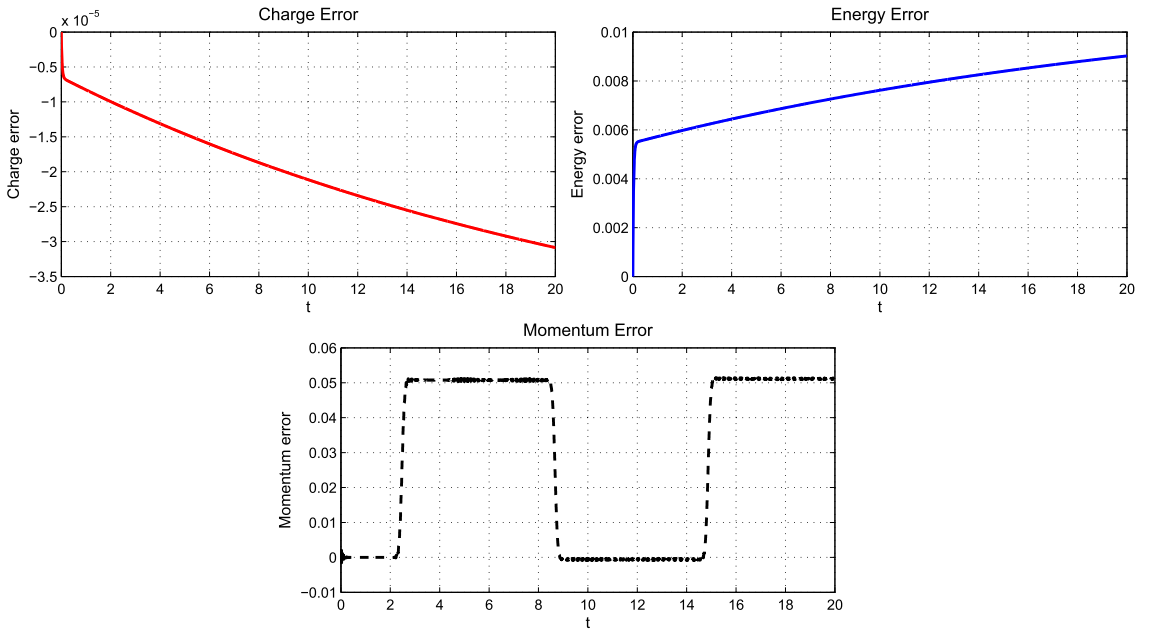

Fig. 6.16. Errors of three invariants of the double soliton of nonlinear Schrödinger equation by the 2-degree DG method with fluxes (P^-, Q^-, V^+, W^+) (see also (5.7)) combining the 3-order SSP Runge–Kutta method for time integration, with the step sizes $\Delta x = 0.4$, $\Delta t = 0.001$.

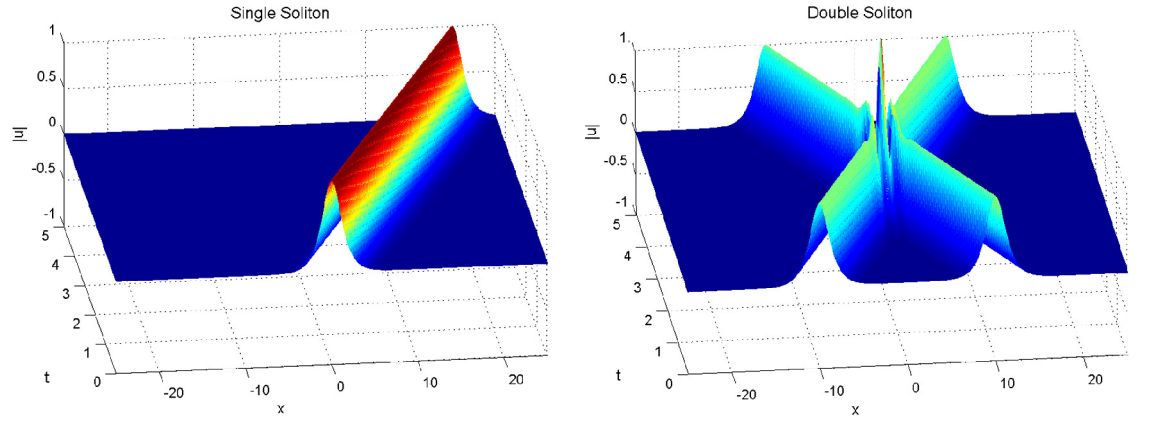

Fig. 6.17. Evolution of single and double soliton solutions by the 2-degree DG method with fluxes (P^-, Q^-, V^+, W^+) (see also (5.7)) combining the implicit midpoint rule for time integration, with the step sizes $\Delta x = 0.4$, $\Delta t = 0.001$.

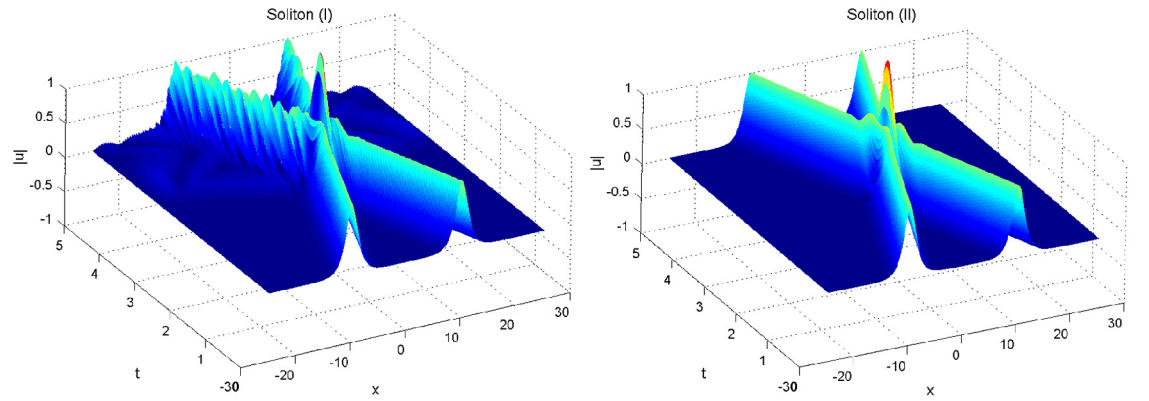

Fig. 6.18. Evolution of double soliton solutions by the 2-degree DG method with the average fluxes $(P^{1/2}, Q^{1/2}, V^{1/2}, W^{1/2})$ (see also (5.22)). The left takes the step sizes $\Delta x = 0.4$, $\Delta t = 0.001$, and the right takes $\Delta x = 0.2$, $\Delta t = 0.001$.

ODEs case. In this paper, the DG approach provides a new way to get the well-defined multi-symplectic integrators as we can get an ODEs after semi-discretizing the Hamiltonian PDEs by DG scheme. It also states that the resulting discretizations derived by applying the DG approach to the system with special structures can preserve the corresponding structure of the original system via choosing appropriate numerical fluxes. Nevertheless, for the lack of the backward error analysis the excellent numerical results of the multi-symplectic numerical methods have not been understood completely [18].

Acknowledgements

We would like to express our sincere gratitude to the referees for their constructive comments which help us to improve the presentation of this paper. The first author was supported by the Foundation of the NNSFC (No. 11401055) and the Foundation of Education Department of Hunan Province (No. 15C0028). The second author was supported by the Foundation of the NNSFC (No. 11271357), the Foundation for Innovative Research Groups of the NNSFC (No. 11321061) and ITER-China Program (No. 2014GB124005).

Appendix. Derivation of continuous-stage PRK method from DG scheme

In this appendix, we show the details of obtaining the continuous-stage PRK scheme (3.7) from the DG method (3.2) with the flux (3.3).

It is known from (3.3) that

$$\widehat{\boldsymbol{P}}_{j+1} = \boldsymbol{P}(t_{j+1}^-), \quad \widehat{\boldsymbol{Q}}_j = \boldsymbol{Q}(t_j^+).$$

By changing the coordinates from t to $\tau \in [0,1]$ with $t = t_j + \tau\Delta t$, it follows from the first formula of (3.2) that

$$\begin{cases} \int_0^1 [\boldsymbol{P}\cdot\phi'(\tau) + \Delta t\, \boldsymbol{f}(\boldsymbol{P},\boldsymbol{Q})\cdot\phi(\tau)]\,\mathrm{d}\tau = \widehat{\boldsymbol{P}}_{j+1}\cdot\phi(1^-) - \widehat{\boldsymbol{P}}_j\cdot\phi(0^+), \\ \widehat{\boldsymbol{P}}_{j+1} = \boldsymbol{P}(t_{j+1}^-) = \boldsymbol{P}(t_j+\tau\Delta t)|_{\tau=1^-} \end{cases} \tag{7.1}$$

which holds for $\phi(\tau) \in \mathbb{P}^k([0,1])$, $j = 0, 1, \cdots, N-1$. Here we use the prime to stand for the derivative with respect to τ. By using the Legendre polynomial $\rho_j(\tau)$ given in (3.6), we expand $\boldsymbol{P}(t_j+\tau\Delta t)$ as

$$\boldsymbol{P}(t_j+\tau\Delta t) = \sum_{\iota=0}^{k} \boldsymbol{\lambda}_\iota \rho_\iota(\tau),\ \boldsymbol{\lambda}_\iota \in \mathbb{R}^d, \tau \in [0,1]. \tag{7.2}$$

We choose the test functions as

$$\phi = 1, \int_0^\tau \rho_0(x)\mathrm{d}x, \cdots, \int_0^\tau \rho_{k-1}(x)\mathrm{d}x,$$

and substitute them into (7.1). Using (7.2) and the orthogonality of Legendre polynomials, it gives

$$\begin{aligned} &\widehat{\boldsymbol{P}}_{j+1} = \widehat{\boldsymbol{P}}_j + \Delta t \int_0^1 \boldsymbol{f}(\boldsymbol{P}(t_j+\tau\Delta t), \boldsymbol{Q}(t_j+\tau\Delta t))\,\mathrm{d}\tau, \\ &\boldsymbol{\lambda}_\iota = -\Delta t \int_0^1 \left[\int_0^\sigma \rho_\iota(x)\mathrm{d}x\, \boldsymbol{f}(\boldsymbol{P}(t_j+\sigma\Delta t), \boldsymbol{Q}(t_j+\sigma\Delta t))\right]\mathrm{d}\sigma + \widehat{\boldsymbol{P}}_{j+1}\delta_{\iota 0}, \quad \iota = 0, \cdots, k-1, \end{aligned} \tag{7.3}$$

where δ_{ij} is the Kronecker symbol. Since

$$\widehat{\boldsymbol{P}}_{j+1} = \boldsymbol{P}(t_j+\tau h)|_{\tau=1^-} = \sum_{\iota=0}^{k} \boldsymbol{\lambda}_\iota \rho_\iota(1) = \sum_{\iota=0}^{k} \boldsymbol{\lambda}_\iota \sqrt{2\iota+1},$$

then it yields

$$\boldsymbol{\lambda}_k = \frac{\widehat{\boldsymbol{P}}_{j+1} - \sum_{\iota=0}^{k-1} \boldsymbol{\lambda}_\iota \sqrt{2\iota+1}}{\sqrt{2k+1}}. \tag{7.4}$$

One can easily get the first formula of (3.7) by substituting $\boldsymbol{\lambda}_\iota$ into (7.2). The third formula of (3.7) is given by the first formula of (7.3).

To get the other two formulae of (3.7), we consider the following formulation

$$\begin{cases} \int_0^1 [\boldsymbol{Q}'\cdot\psi(\tau) - \Delta t\boldsymbol{g}(\boldsymbol{P},\boldsymbol{Q})\cdot\psi(\tau)]\,\mathrm{d}\tau = [\boldsymbol{Q}(t_{j+1}^-) - \widehat{\boldsymbol{Q}}_{j+1}]\cdot\psi(1^-), \\ \widehat{\boldsymbol{Q}}_j = \boldsymbol{Q}(t_j^+) = \boldsymbol{Q}(t_j+\tau\Delta t)|_{\tau=0^+} \end{cases} \tag{7.5}$$

which holds for all $\psi(\tau)\in\mathbb{P}^k([0,1])$, $j=0,1,\cdots,N-1$. Here, the first formula of (7.5) is deduced from the second formula of (3.2) with the help of integration by parts.

Now we use the following expansion

$$\boldsymbol{Q}'(t_j+\tau\Delta t) = \sum_{\iota=0}^{k-1}\boldsymbol{\gamma}_\iota\rho_\iota(\tau),\ \boldsymbol{\gamma}_\iota\in\mathbb{R}^d,\tau\in[0,1] \tag{7.6}$$

and choose the test functions,respectively, as

$$\psi = \rho_0(\tau),\rho_1(\tau),\cdots,\rho_k(\tau).$$

By inserting them into (7.5), using (7.6) and the orthogonality of $\{\rho_l(\tau)\}_{l\geq 0}$ gives

$$\boldsymbol{\gamma}_\iota = \Delta t\int_0^1 \boldsymbol{g}(\boldsymbol{P}(t_j+\sigma\Delta t),\boldsymbol{Q}(t_j+\sigma\Delta t))\rho_\iota(\sigma)\,\mathrm{d}\sigma + (\boldsymbol{Q}(t_{j+1}^-) - \widehat{\boldsymbol{Q}}_{j+1})\sqrt{2\iota+1} \tag{7.7}$$

for $\iota=0,\cdots,k-1$, and

$$\Delta t\int_0^1 \boldsymbol{g}(\boldsymbol{P}(t_j+\sigma\Delta t),\boldsymbol{Q}(t_j+\sigma\Delta t))\rho_k(\sigma)\,\mathrm{d}\sigma = -(\boldsymbol{Q}(t_{j+1}^-) - \widehat{\boldsymbol{Q}}_{j+1})\sqrt{2k+1}.$$

This leads to

$$\boldsymbol{Q}(t_{j+1}^-) - \widehat{\boldsymbol{Q}}_{j+1} = -\frac{1}{\sqrt{2k+1}}\Delta t\int_0^1 \boldsymbol{g}(\boldsymbol{P}(t_j+\sigma\Delta t),\boldsymbol{Q}(t_j+\sigma\Delta t))\rho_k(\sigma)\,\mathrm{d}\sigma. \tag{7.8}$$

Substituting (7.8) into (7.7) gives

$$\boldsymbol{\gamma}_\iota = \Delta t\int_0^1 [(\rho_\iota(\sigma) - \frac{\sqrt{2\iota+1}}{\sqrt{2k+1}}\rho_k(\sigma))\boldsymbol{g}(\boldsymbol{P}(t_j+\sigma\Delta t),\boldsymbol{Q}(t_j+\sigma\Delta t))]\,\mathrm{d}\sigma,\ \iota=0,\cdots,k-1.$$

Integrating (7.6) from 0 to τ, it follows that

$$\begin{aligned} \boldsymbol{Q}(t_j+\tau\Delta t) &= \boldsymbol{Q}(t_j^+) + \sum_{\iota=0}^{k-1}\boldsymbol{\gamma}_\iota\int_0^\tau \rho_\iota(x)\,\mathrm{d}x \\ &= \widehat{\boldsymbol{Q}}_j + \sum_{\iota=0}^{k-1}\boldsymbol{\gamma}_\iota\int_0^\tau \rho_\iota(x)\,\mathrm{d}x. \end{aligned} \tag{7.9}$$

By inserting $\boldsymbol{\gamma}_\iota$ into the above formula, we derive the second formula of (3.7). The last formula of (3.7) can be deduced by using (7.8) and (7.9).

Similarly, the DG method with flux (3.4) can also be considered as a continuous-stage PRK scheme.

References

[1] P. Betsch, P. Steinmann, Inherently energy conserving time finite elements for classical mechanics, J. Comput. Phys. 160 (2000) 88–116.
[2] M. Borri, C. Bottasso, A general framework for interpreting time finite element formulations, Comput. Mech. 13 (1993) 133–142.
[3] C.L. Bottasso, A new look at finite elements in time: a variational interpretation of Runge–Kutta methods, Appl. Numer. Math. 25 (1997) 355–368.
[4] T.J. Bridges, S. Reich, Multi-symplectic integrators: numerical schemes for Hamiltonian PDEs that conserve symplecticity, Phys. Lett. A 284 (2001) 184–193.
[5] C. Chen, Q. Tang, Continuous finite element methods for Hamiltonian systems, Appl. Math. Mech. 28 (8) (2007) 1071–1080.
[6] J. Chen, Multisymplectic geometry, local conservation laws and Fourier pseudospectral discretization for the "good" Boussinesq equation, Appl. Math. Comput. 161 (1) (2005) 55–67.
[7] B. Cockburn, C.-W. Shu, Runge–Kutta discontinuous Galerkin methods for convection-dominated problems, J. Sci. Comput. 16 (3) (2001) 173–261.

[8] R. de Vogelaere, Methods of Integration which Preserve the Contact Transformation Property of the Hamiltonian Equations, Report, Department of Mathematics, University of Notre Dame, 1956, p. 4.
[9] K. Feng, On difference schemes and symplectic geometry, in: Proceedings of the 5-th Inter., Symposium of Differential Geometry and Differential Equations, Beijing, 1984, pp. 42–58.
[10] E. Hairer, C. Lubich, G. Wanner, Geometric Numerical Integration: Structure-Preserving Algorithms For Ordinary Differential Equations, second edition, Springer Ser. Comput. Math., vol. 31, Springer-Verlag, Berlin, 2006.
[11] E. Hairer, Energy-preserving variant of collocation methods, J. Numer. Anal. Ind. Appl. Math. 5 (2010) 73–84.
[12] J. Hong, H. Liu, G. Sun, The multi-symplecticity of partitioned Runge–Kutta methods for Hamiltonian PDEs, Math. Comput. 75 (253) (2005) 167–181.
[13] J. Hong, A survey of multi-symplectic Runge–Kutta type methods for Hamiltonian partial differential equations, in: Frontiers and Prospects of Contemporary Applied Mathematics, 2005, pp. 71–113.
[14] R.A. Horn, C.R. Johnson, Matrix Analysis, second edition, Cambridge University Press, 2013.
[15] B.L. Hulme, Discrete Galerkin and related one-step methods for ordinary differential equations, Math. Comput. 26 (1972) 881–891.
[16] A.L. Islas, D.A. Karpeev, C.M. Schober, Geometric integrators for the nonlinear Schrödinger equation, J. Comput. Phys. 173 (1) (2001) 116–148.
[17] Y. Li, X. Wu, Functionally fitted energy-preserving methods for solving oscillatory nonlinear Hamiltonian systems, SIAM J. Numer. Anal. 54 (4) (2016) 2036–2059.
[18] R.I. McLachlan, B.N. Ryland, Y. Sun, High order multisymplectic Runge–Kutta methods, SIAM J. Sci. Comput. 36 (5) (2014) 2199–2226.
[19] J.E. Marsden, G.W. Patrick, S. Shkoller, Multi-symplectic geometry, variational integrators, and nonlinear PDEs, Commun. Math. Phys. 199 (1998) 351–395.
[20] M. Qin, M. Zhang, Multi-stage symplectic schemes of two kinds of Hamiltonian systems for wave equations, Comput. Math. Appl. 19 (1990) 51–62.
[21] W.H. Reed, T.R. Hill, Triangular Mesh Methods for the Neutron Transport Equation, Tech. report LA-UR-73-479, Los Alamos Scientific Laboratory, 1973.
[22] S. Reich, Multi-symplectic Runge–Kutta collocation methods for Hamiltonian wave equations, J. Comput. Phys. 157 (2000) 473–499.
[23] B.N. Ryland, R.I. Mclachlan, On Multisymplecticity of partitioned Runge–Kutta methods, SIAM J. Sci. Comput. 30 (3) (2008) 1318–1340.
[24] C.-W. Shu, A survey of strong stability preserving high order time discretizations, Collect. Lect. Preserv. Stab. Discret. 109 (2002) 51–65.
[25] C.W. Shu, Discontinuous Galerkin methods: general approach and stability, in: Numerical Solutions of Partial Differential Equations, 2009, pp. 149–201.
[26] G. Sun, Construction of high order symplectic PRK methods, J. Comput. Math. 13 (1) (1995) 40–50.
[27] Y. Sun, Quadratic invariants and multi-symplecticity of partitioned Runge–Kutta methods for Hamiltonian PDEs, Numer. Math. 106 (2007) 691–715.
[28] W. Tang, Y. Sun, A new approach to construct Runge–Kutta type methods and geometric numerical integrators, AIP Conf. Proc. 1479 (2012) 1291–1294.
[29] W. Tang, Y. Sun, Time finite element methods: a unified framework for numerical discretizations of ODEs, Appl. Math. Comput. 219 (2012) 2158–2179.
[30] W. Tang, G. Lang, X. Luo, Construction of symplectic (partitioned) Runge–Kutta methods with continuous stage, Appl. Math. Comput. 286 (2016) 279–287.
[31] W. Tang, Y. Sun, Construction of Runge–Kutta type methods for solving ordinary differential equations, Appl. Math. Comput. 234 (2014) 179–191.
[32] Y. Wang, B. Wang, M. Qin, Numerical implementation of the multisymplectic Preissman scheme and its equivalent schemes, Appl. Math. Comput. 149 (2004) 299–326.
[33] Y. Xu, C.W. Shu, Local discontinuous Galerkin methods for nonlinear Schrödinger equations, J. Comput. Phys. 205 (2005) 72–97.
[34] J. Yan, C.-W. Shu, Local discontinuous Galerkin methods for partial differential equations with higher order derivatives, J. Sci. Comput. 17 (2002) 27–47.